



EASTLAND PORT MAINTENANCE DREDGING AND DISPOSAL PROJECT

Surfing wave dynamics at Midway Beach, Gisborne

Report prepared for Eastland Port Limited

August 2018

Meteorological Service New Zealand Ltd: P0331-12

August 2018

Report status

Version	Date	Status	Approved by
RevA	16/08/2018	Draft for internal review	Weppe
RevB	17/08/2018	Draft for client review	Beamsley
RevC	22/08/2018	Updated draft for client review	Beamsley

The information, including the intellectual property, contained in this report is confidential and proprietary to Meteorological Service New Zealand Ltd. It may be used by the persons to whom it is provided for the stated purpose for which it is provided, and must not be imparted to any third person without the prior written approval of Meteorological Service New Zealand Ltd. Meteorological Service New Zealand Ltd reserves all legal rights and remedies in relation to any infringement of its rights in respect of its confidential information.

TABLE OF CONTENTS

1.	Introduction	5
2.	Methods	8
	2.1. Wave hindcast.....	8
	2.2. Surfing wave climate analysis	10
	2.3. Numerical nearshore wave modelling.....	10
3.	Results	13
	3.1. General and surfing wave climate	13
	3.2. Nearshore wave modelling	21
	3.2.1. Big River	21
	3.2.2. Pipe and Roberts Road.....	28
4.	Conclusions.....	36
5.	References.....	37

LIST OF FIGURES

Figure 1.1	Maps showing the location of Poverty Bay (a and b), and Eastland Port (c) with the locations used in the present study. Both offshore disposal and shipping channel are indicated on top of the bathymetry in (d).6
Figure 1.2	Location of the Nationally and regionally significant surf breaks within Poverty Bay.7
Figure 2.1	Map showing the nested SWAN domains used to simulate the spectral transformation of the offshore wave climates to the nearshore zone. Information specific to each set-up is provided in Table 2.1.9
Figure 2.2	SWASH model domain extents and bathymetry (top). The domain is 900x700 grid cells with a spatial resolution of 5 m. Wave conditions were applied to the southern and eastern boundaries; the northern boundary was set as a radiation boundary. The model domain includes a sponge layer of 500 m wide (~4-5 wave lengths) to the west of the domain so that waves propagate out of the domain without reflection. The red dots indicate the position where wave data was extracted for the wave climate analysis (southern model boundary) and Midway Beach. The bottom plot shows depth difference between the existing and post-dredging scenarios. Positive depth difference means deeper water on the post-dredging scenario. 12
Figure 3.1.	Snapshot of significant wave height from the NZN (res. 4km) and Gisborne (res. 500m) domains during swell events with southwest and northeast offshore directions. Note the different degrees of exposure to wave energy in the Bay of Poverty. 14
Figure 3.2.	Snapshot of significant wave height from the NZN (res. 4km), Gisborne (res. 500m), and Poverty Bay (res. 80m) SWAN domains for a large southwest swell event (29 June 2012). The black rectangles show the successive nested domains. 15
Figure 3.3.	Mean wave rose over the 10 year time-series showing the distribution of significant wave heights and peak directions. Associated joint probabilities are provided in Table 3.1. 16
Figure 3.4.	Mean wave rose over the 10 year time-series showing the distribution of significant swell wave heights and peak directions. Associated joint probabilities are provided in Table 3.2. 16
Figure 3.5.	Mean wind rose over the 10 year time-series showing the distribution of significant wind speed and directions. 17
Figure 3.6.	Wave rose for favourable surfing conditions during the 10 year time-series showing the distribution of significant swell wave heights and peak directions. Associated joint probabilities are provided in Table 3.3. 18
Figure 3.7.	Wave rose for favourable surfing conditions during the 10 year time-series showing the distribution of peak periods and peak directions. Associated joint probabilities are provided in Table 3.4. 18
Figure 3.8	Post-disposal significant wave height (top) and difference in significant wave height (bottom) caused by the 4.4 cm disposal mound for the wave class 1. 22
Figure 3.9	Post-disposal significant wave height (top) and difference in significant wave height (bottom) caused by the 4.4 cm disposal mound for the wave class 2. 23
Figure 3.10	Post-disposal significant wave height (top) and difference in significant wave height (bottom) caused by the 4.4 cm disposal mound for the wave class 3. 24

Figure 3.11	Post-disposal significant wave height (top) and difference in significant wave height (bottom) caused by the 4.4 cm disposal mound for the wave class 4.	25
Figure 3.12	Post-disposal significant wave height (top) and difference in significant wave height (bottom) caused by the 4.4 cm disposal mound for the wave class 5.	26
Figure 3.13	Post-disposal significant wave height (top) and difference in significant wave height (bottom) caused by the 4.4 cm disposal mound for the wave class 6.	27
Figure 3.14	Snapshots of sea surface elevation (top) and significant wave height field (bottom) predicted for idealized monochromatic wave conditions $H_s = 2.0\text{m}$, $T_p = 12 \text{ sec.}$ and $D_p = 140^\circ\text{T}$, over the existing bathymetry. The channel footprint is shown as a white polygon. The Midway Beach area is shown by the red dot.	30
Figure 3.15	Snapshots of sea surface elevation (top) and significant wave height field (bottom) predicted for idealized monochromatic wave conditions $H_s = 2.0\text{m}$, $T_p = 12 \text{ sec.}$ and $D_p = 150^\circ\text{T}$, over the existing bathymetry. The channel footprint is shown as a white polygon. The Midway Beach area is shown by the red dot.	31
Figure 3.16	Snapshots of sea surface elevation (top) and significant wave height field (bottom) predicted for idealized monochromatic wave conditions $H_s = 2.0\text{m}$, $T_p = 12 \text{ sec.}$ and $D_p = 160^\circ\text{T}$, over the existing bathymetry. The channel footprint is shown as a white polygon. The Midway Beach area is shown by the red dot.	32
Figure 3.17	Snapshots of sea surface elevation (top) and significant wave height field (bottom) predicted for idealized monochromatic wave conditions $H_s = 2.0\text{m}$, $T_p = 12 \text{ sec.}$ and $D_p = 170^\circ\text{T}$, over the existing bathymetry. The channel footprint is shown as a white polygon. The Midway Beach area is shown by the red dot.	33
Figure 3.18	Snapshots of sea surface elevation (top) and significant wave height field (bottom) predicted for idealized spectral wave conditions $H_s = 2.0\text{m}$, $T_p = 12 \text{ sec.}$ and $D_p = 150^\circ\text{T}$, over the existing bathymetry. The channel footprint is shown as a white polygon. The Midway Beach area is shown by the red dot.	34
Figure 3.28	Snapshots of sea surface elevation (top) and significant wave height field (bottom) predicted for idealized spectral wave conditions $H_s = 2.0\text{m}$, $T_p = 12 \text{ sec.}$ and $D_p = 160^\circ\text{T}$, over the existing bathymetry. The channel footprint is shown as a white polygon. The Midway Beach area is shown by the red dot.	35

LIST OF TABLES

Table 2.1	Extents, resolution and frequency range defined for the four SWAN nests. Each child domain was run off spectral wave boundaries provided by the domain immediately above in the table. Spectral boundaries to run the NZN parent nest were prescribed from the 0.5° global WW3 wave model.	9
Table 3.1	Joint probabilities of significant wave heights and peak wave directions during the 10 year study period.	19
Table 3.2	Joint probabilities of significant swell wave heights (period>8 seconds) and peak wave directions during the 10 year study period.	19
Table 3.3	Joint probabilities of significant swell wave heights and peak wave directions during good surfing conditions (see surfing conditions criteria's in section 2.2).	19
Table 3.4	Joint probabilities of peak wave period and peak wave directions during good surfing conditions (see surfing conditions criteria's in section 2.2).	20

1. INTRODUCTION

Eastland Port Ltd are seeking to renew their maintenance dredging and disposal consents at the Port of Gisborne.

Currently, dredged sediment is disposed at an offshore disposal site situated in approximately 18 – 20 m water depth (Figure 1.1), with an average annual rate of approximately 73,000 m³ based on estimates obtained between 2002 and 2019 by Eastland Port.

Maintenance dredging is expected to occur using the Trailing Suction Hopper Dredge (TSHD) “Pukunui” although, if there are significant inflows of sediment due to large storm events, a higher productivity Trailing Suction Hopper Dredge (TSHD) may be required to ensure the required port and channel depths can be maintained. It is likely that some maintenance dredging may also be undertaken using a Backhoe Dredger (BHD) or Cutter Suction Dredger (CSD).

MetOcean Solutions (MOS) has been contracted to provide coastal oceanographic expertise to investigate both physical and morphological effects and associated sediment transport patterns resulting from the dredging and disposal of maintenance dredging material at the current disposal site.

The primary objective of this study is to assess the effects of the Eastland Port maintenance dredging and disposal on the existing nearshore wave processes in the Poverty Bay and specifically how it may affect the resulting surfable wave conditions. The study includes an assessment of the general and surfing-related wave climates and numerical modelling of nearshore wave propagation within Poverty Bay.

Within Poverty Bay there are both nationally (Bowl – Tuamotu Island) and regionally significant surf breaks (Pipe, Roberts Road, Big River, Sponge Bay, The Cliffs), with the locations of the breaks, relative to the shipping channel and offshore disposal ground, given in Figure 1.2. Also shown in Figure 1.2 is the approximate offshore incident wave direction (see MetOcean Solutions, 2017). Of the Nationally and regionally significant surf breaks within Poverty Bay, only Roberts Road, Pipe and Big River have the potential of being effected by the continuation of the maintenance dredging activities. The remaining breaks are offshore of the proposed developments and will not be impacted.

Both Roberts Road and Pipe are classified as beach breaks and rely on pre-conditioning of the incident wave field to generated the well-known peaked surf breaks (see Beamsley and Black, 2003). In contrast, Big River at the mouth of the Waipaoa River is considered a fickle spot that features both left and right river bar peak, with the banks controlled by the high volume river which creates consistently moving sand and shingle banks (Morse and Brunskill, 2004), and is not reliant on any pre-conditioning of the incoming wave field.

The report focuses on the surf breaks potentially affected by the proposed activities (Roberts Road, Pipe and Big River, Figure 1.2.), and is structured as follows; details of the adopted methodology for identifying suitable surfing events, along with the numerical modelling approach applied is provided in Section 2. Key results are provided in Section 3, while a brief summary of the findings is given in Section 4. Cited references are provided in Section 5.

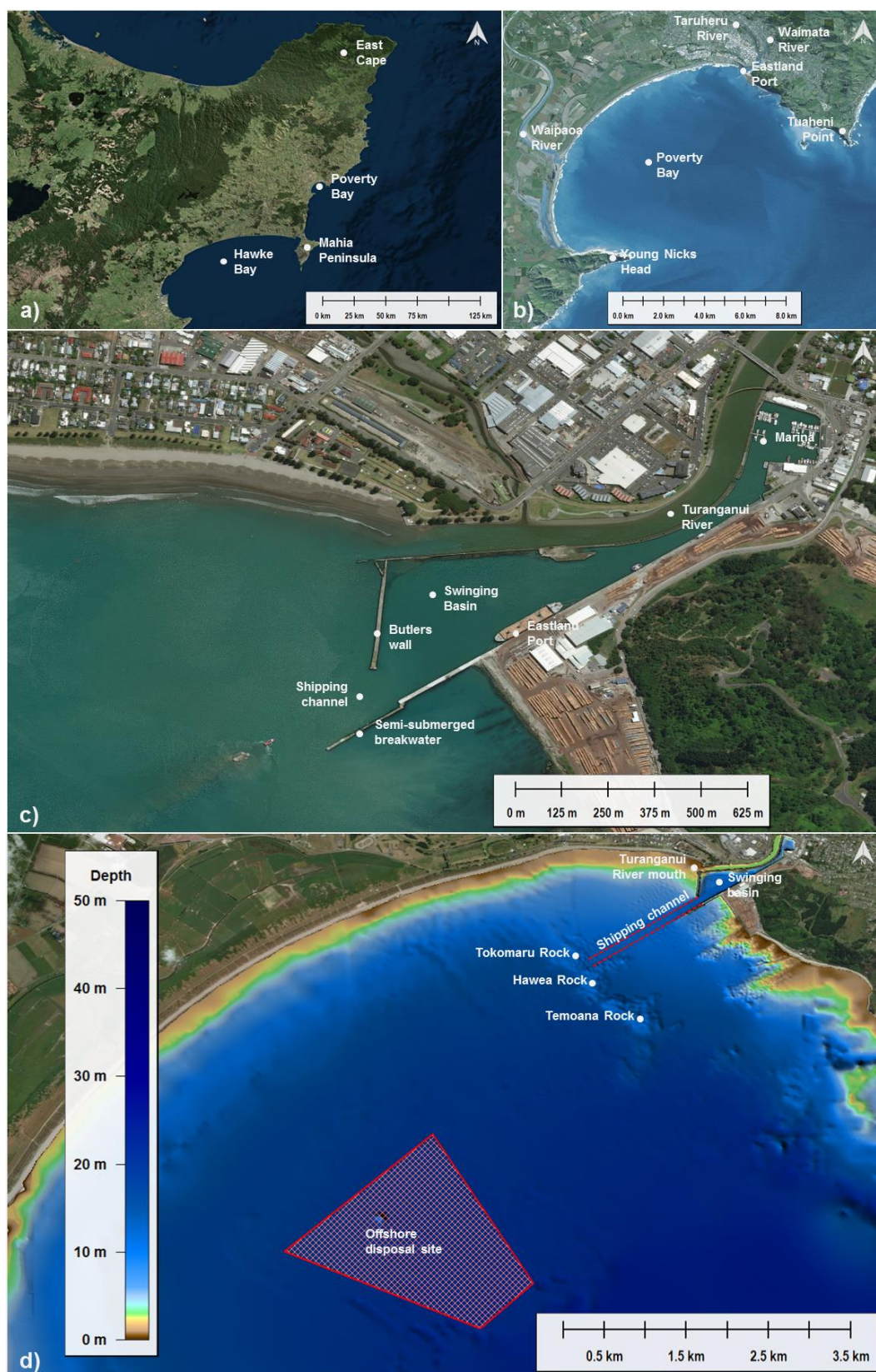


Figure 1.1 Maps showing the location of Poverty Bay (a and b), and Eastland Port (c) with the locations used in the present study. Both offshore disposal and shipping channel are indicated on top of the bathymetry in (d).



Figure 1.2 Location of the Nationally and regionally significant surf breaks within Poverty Bay.

2. METHODS

2.1. Wave hindcast

The wave climate assessment is based on the analysis of high-resolution wave hindcast produced in a previous study P0331-05 (MetOcean Solutions, 2017).

Wave modelling was undertaken using a modified version of SWAN¹, calibrated over years 2007 and 2008 and used to run a high-resolution, 10-year hindcast of the Poverty Bay region spanning 1996 to 2005. Validation details are available in P0331-05 (MetOcean Solutions, 2017).

SWAN is a third generation ocean wave propagation model which solves the spectral action density balance equation. The model simulates the growth, refraction and decay of each frequency-direction component of the complete sea state, providing a realistic description of the wave field as it changes in time and space. Physical processes that are modelled include the generation of waves by surface wind, dissipation by white-capping, resonant nonlinear interaction between the wave components, bottom friction and depth limited wave breaking energy dissipation.

A detailed description of the model equations, parameterisations and numerical schemes can be found in Holthuijsen (2007) or the SWAN documentation².

In the present implementation, SWAN was run in the non-stationary mode with all third generation physics included in the model. The source term parameterisations of Van der Westhuysen et al. (2007) were employed and the Collins (1972) scheme was used for bottom friction. The spectra were discretised with 36 directional bins (10° directional resolution) and logarithmic frequencies starting at 0.0412 Hz and extending up to 1.4003 Hz for the highest resolution nests (see Table 2.1), with resolution $df = 0.1f$.

A downscale nesting approach was employed to resolve the nearshore region around Eastland Port (Figure 2.1). Four regular nests were defined with resolutions progressively increasing from of 4 km and 20 m (Table 2.1).

A regional atmospheric hindcast using the Weather and Research Forecasting (WRF) was used to provide atmospheric forcings to SWAN. The WRF dataset was run over New Zealand at approximately 12 km resolution. Boundary conditions were derived from the global Climate Forecast System Reanalysis (CFSR)³. This leap of resolution from the 35 km available from CFSR (23 km after 2011) adds accuracy and variability to the atmospheric fields that force the wave model.

Full spectral boundaries for the coarser SWAN domain were prescribed from a global implementation of WAVEWATCH III (WW3) spectral wave model (Tolman, 1991) run at 0.5° resolution using the source term parameterisations of Ardhuin et al. (2010).

¹ Modified from SWAN version of the 40.91 release

² http://swanmodel.sourceforge.net/online_doc/online_doc.htm

³ <https://climatedataguide.ucar.edu/climate-data/climate-forecast-system-reanalysis-cfsr>

Table 2.1 Extents, resolution and frequency range defined for the four SWAN nests. Each child domain was run off spectral wave boundaries provided by the domain immediately above in the table. Spectral boundaries to run the NZN parent nest were prescribed from the 0.5° global WW3 wave model.

Domain	Longitude (degree)			Latitude (degree)			Frequencies (Hz)	
	West	East	Res	South	North	Res	Lowest	Highest
NZN	170.00	180.00	0.0400	-43.000	-34.0000	0.0400	0.0412	0.7186
Gisborne	177.75	178.50	0.0050	-39.330	-38.5800	0.0050	0.0412	1.0521
Poverty Bay	177.93	178.11	0.0008	-38.780	-38.6696	0.0008	0.0412	1.4003
Eastland	178.00	178.05	0.0002	-38.704	-38.6696	0.0008	0.0412	1.4003

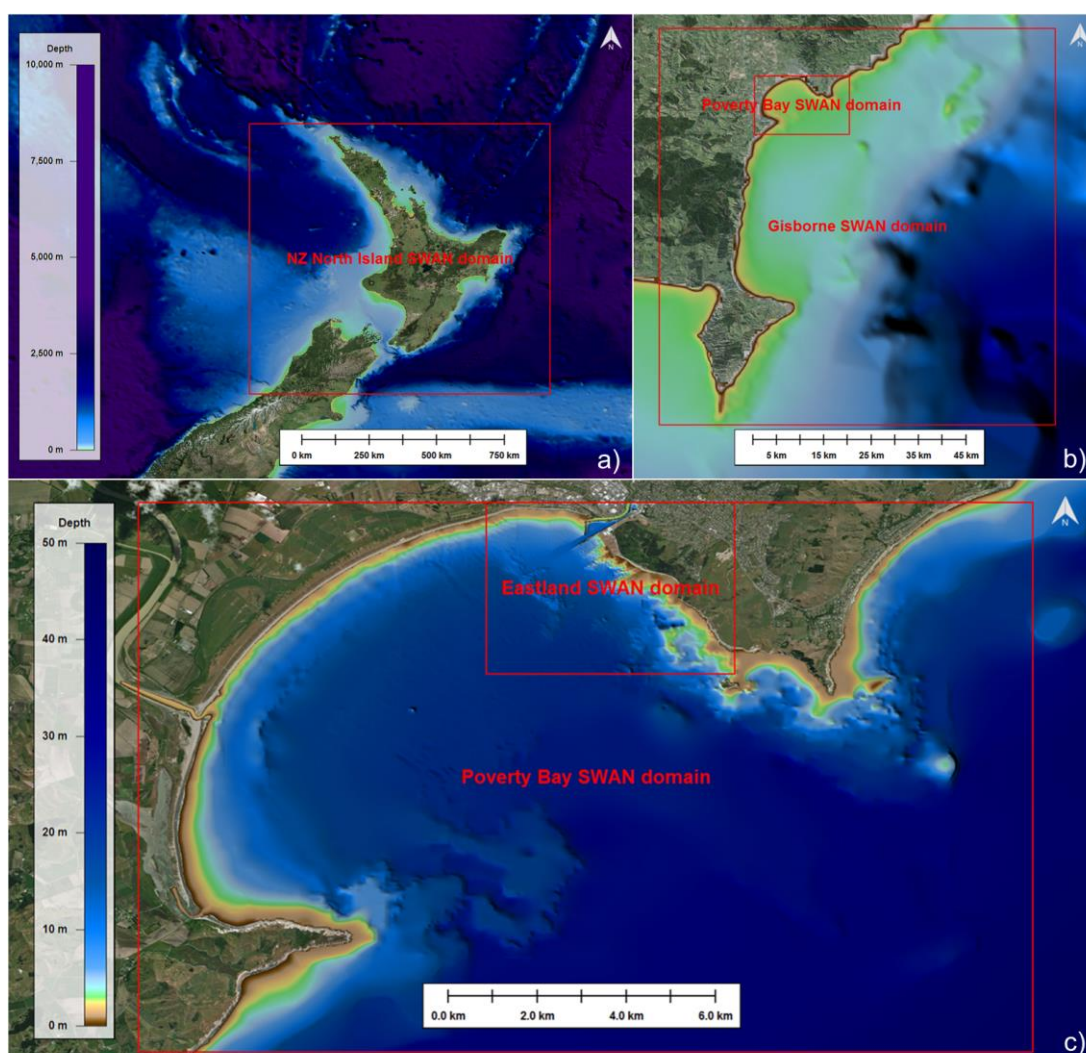


Figure 2.1 Map showing the nested SWAN domains used to simulate the spectral transformation of the offshore wave climates to the nearshore zone. Information specific to each set-up is provided in Table 2.1.

2.2. Surfing wave climate analysis

The analysis of the wave climate focused on the determination of the general features and occurrence of swell-dominated surfing events. The reference location used for the analysis was located off the Midway Beach (see Figure 2.2). Conditions offshore Midway Beach are considered to be representative of the breaks within Poverty Bay potentially impacted by the maintenance dredging (i.e. Roberts Road, Pipe and Big River), though recognising that wave directions at Big River are likely to be orientated slightly more eastward due to wave refraction processes within the bay.

It is acknowledged that locally generated short-period wave events (i.e. events with periods less than 11 seconds) may also be conducive of favourable surfing conditions at the adjacent surfing beaches. As refraction processes are dependent on wave period, wave events with periods of <11 seconds will experience a proportionately smaller degree of refraction than events with longer wave periods. Therefore, considering events with 11 second and higher incident wave periods focuses on events or conditions that will experience the most significant potential change in inshore surfing conditions.

The swell-dominated conditions expected to be favourable for surfing were defined as follow:

- Significant swell wave height larger than 1.0 metre
- Peak period larger than 11.0 seconds
- Incident peak wave direction from the 90-270 degrees window.
- Wind speeds smaller than 10 knots regardless of direction, or
- Wind direction from the 315-45 degrees window (i.e. approximately off to cross-offshore for considered spot).
- Wave events fulfilling the above conditions for at least 6 hours.

The results were used to define a range of idealised surfing events that were used as reference to assess the relative effects of the Eastland Port maintenance dredging.

2.3. Numerical nearshore wave modelling

For the surf break Big River the impact of the proposed disposal mound (maintenance) on the inshore wave characteristics has been assessed using the phase-averaging SWAN model (detailed in Section 2.1 and in MetOcean Solutions, 2018). This is appropriate as the functionality of Big River is dependent on banks controlled by the high volume river which creates consistently moving sand and shingle banks (Morse and Brunskill, 2004), and is not reliant on any pre-conditioning of the incoming wave field.

Where pre-conditioning is important for the functionality of the surf break (i.e. Roberts Road and Pipe) detailed nearshore wave modelling was undertaken using the non-linear wave propagation model SWASH⁴.

SWASH is an open-source non-hydrostatic wave-flow model solving the non-linear shallow water equations including non-hydrostatic pressure. It is intended to be used for predicting transformation of dispersive surface waves from offshore to the beach, for studying the surf zone and swash zone dynamics, wave propagation and agitation in ports and harbours, rapidly varied shallow water flows typically found in coastal flooding resulting from e.g. dike breaks, tsunamis and flood waves, density driven flows in coastal waters, and large-scale ocean circulation, tides and storm surges. A complete description of the numerical algorithms used in the code are provided in Zijlema, M. et al. (2011).

The model simulates individual waves as they propagate over the bathymetry towards the shore (i.e. phase-resolving model). This is of particular interest in a surfing break assessment context as it allows reproducing the evolution of the wave crest patterns as waves propagate towards the coast and identify the wave focusing and crest snapping processes which are very often conducive to high-quality surfing waves (e.g. Aramoana Beach – see MetOcean Solutions Ltd, 2011).

The simulations used a domain of 900 by 700 grid cells with a spatial resolution of 5 m (Figure 2.2.). The existing bathymetry was interpolated from merged bathymetric surveys used in previous study of the area (e.g. P0331-05 MetOcean Solutions, 2017). Both monochromatic and spectral wave conditions were simulated. Wave conditions were applied to the southern and eastern boundaries; the northern boundary was set as a radiation boundary. The model domain includes a sponge layer of 500 m wide (~4-5 wave lengths) to the west of the domain which allows waves to propagate out of the domain without reflection. The model was run in depth-averaged mode accounting for wave breaking using the hydrostatic front approximation (Smit, P. et al., 2013). The domain extents and bathymetry are shown in Figure 2.2.

⁴ <http://swash.sourceforge.net/> , http://swash.sourceforge.net/online_doc/swashuse/swashuse.html

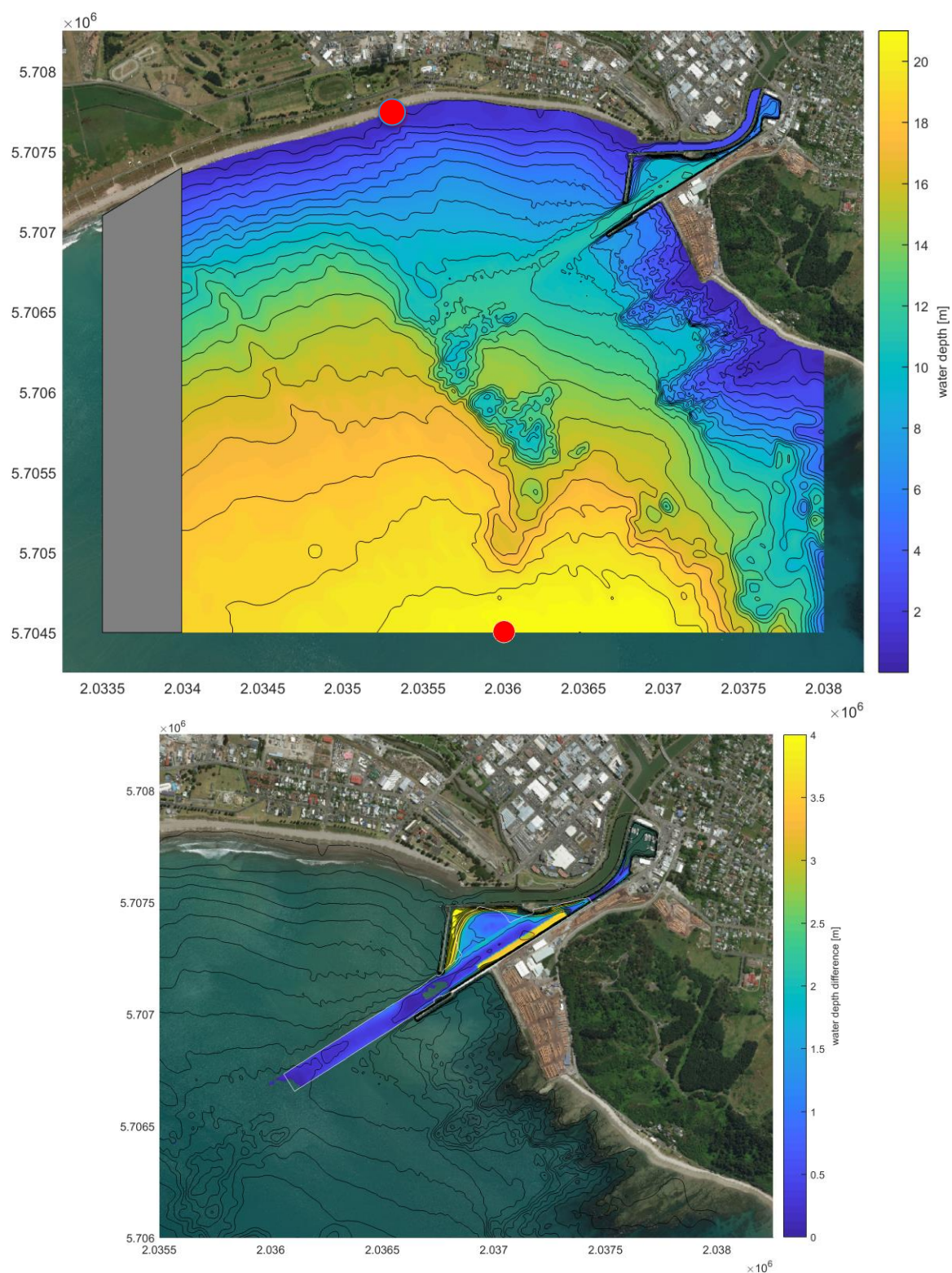


Figure 2.2 SWASH model domain extents and bathymetry (top). The domain is 900x700 grid cells with a spatial resolution of 5 m. Wave conditions were applied to the southern and eastern boundaries; the northern boundary was set as a radiation boundary. The model domain includes a sponge layer of 500 m wide (~4-5 wave lengths) to the west of the domain so that waves propagate out of the domain without reflection. The red dots indicate the position where wave data was extracted for the wave climate analysis (southern model boundary) and Midway Beach. The bottom plot shows depth difference between the existing and post-dredging scenarios. Positive depth difference means deeper water on the post-dredging scenario.

3. RESULTS

3.1. General and surfing wave climate

The present analysis was undertaken using a 10-year series of wave parameters extracted off the Midway Beach area, at the centre of the offshore SWASH domain boundary (see Figure 2.2) from the highest resolution wave hindcast (res. 20 m) described in Section 2.1.

The general wave directional climate off the Midway Beach area is essentially unimodal with a narrow directional range between 140-170° T. This narrow wave exposure window is due to both the general land configuration of NZ North Island, notably the Mahia Peninsula landmass which blocks most pure southerly wave energy events, as well as the Beach position in the northern end of Poverty Bay, and thus sheltered from any east-northeast-incident wave energy by the Tamaru headland. Additionally, the process of refraction around the bay headlands, and diffraction of the wave energy entering the bay acts to further limit the expected directional spreading offshore Midway Beach. This is illustrated in Figure 3.1 showing two swell events with contrasting offshore wave directions.

The typical wave events that do result in significant wave energy at the site consists of offshore southerly swell moving up New Zealand which are refracted by the regional bathymetry off the Poverty Bay to eventually approach the Bay with a SE incidence. A set of wave field snapshots during a large southerly swell event is reproduced from report P0331-05 (MetOcean Solutions, 2017) to illustrate the main wave propagation patterns through the regional and local scales in Figure 3.2.

This narrow directional range is expectedly reproduced in the surf-specific wave climate (Figure 3.6) with a large majority of swell-dominated surfing events in the window 150-160°T (>80 % of the time during good surfing conditions, see Table 3.3). Associated significant swell wave heights are most often in the 1-1.5 m range (~75 % of the time) and less frequently in the 2-3 m range (~6% of time). Most frequent peak periods range from 11 to 15 seconds, with smaller occurrences of longer period wave events (15-18 seconds).

Based on the analysis, idealised surfing wave events with significant wave height of 2.0 meters, peak period of 12.0 seconds and incidence from 140,150,160, and 170° T were considered for the nearshore wave modelling outlined in the following section 3.2.

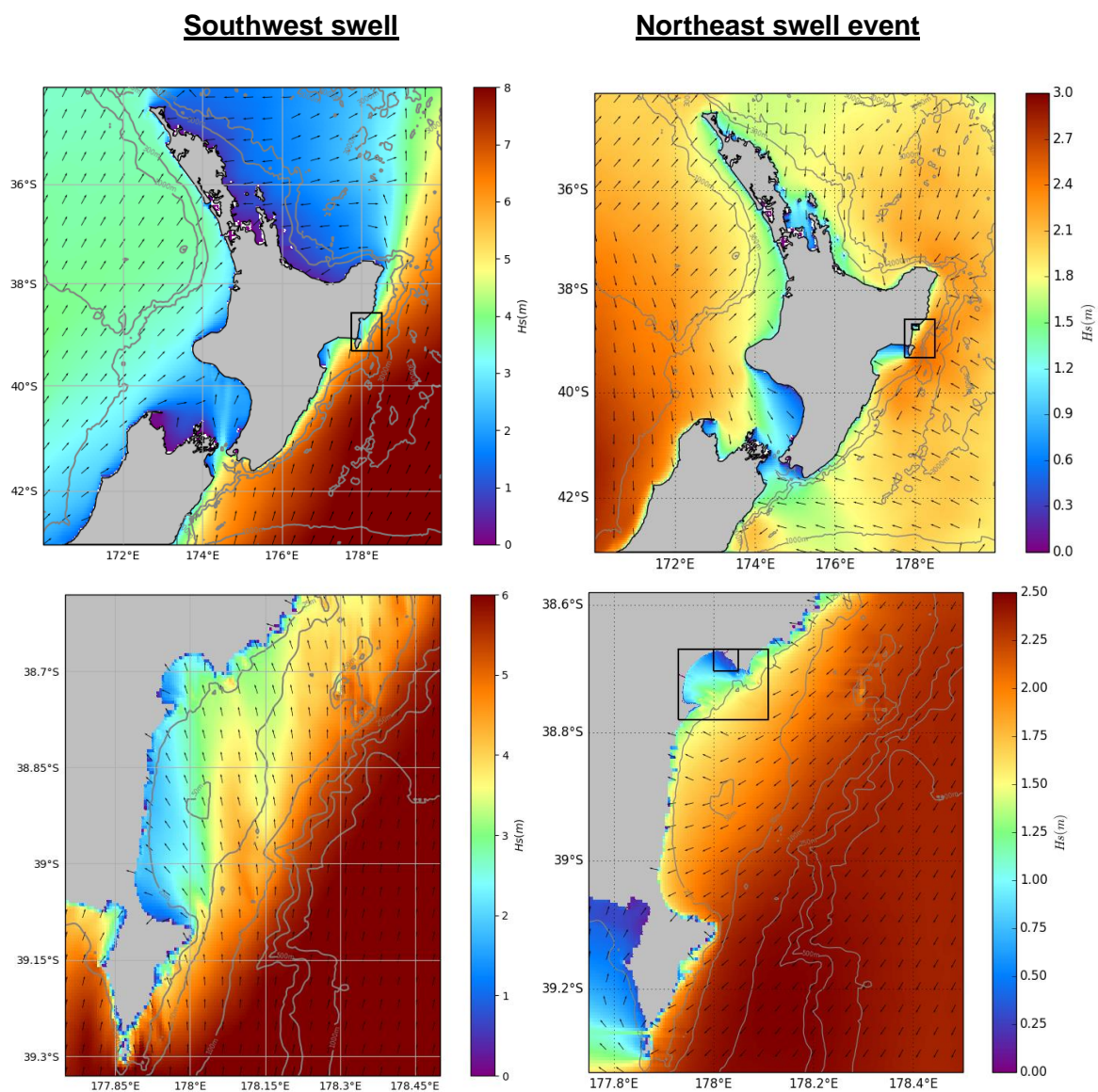


Figure 3.1. Snapshot of significant wave height from the NZN (res. 4km) and Gisborne (res. 500m) domains during swell events with southwest and northeast offshore directions. Note the different degrees of exposure to wave energy in the Bay of Poverty.

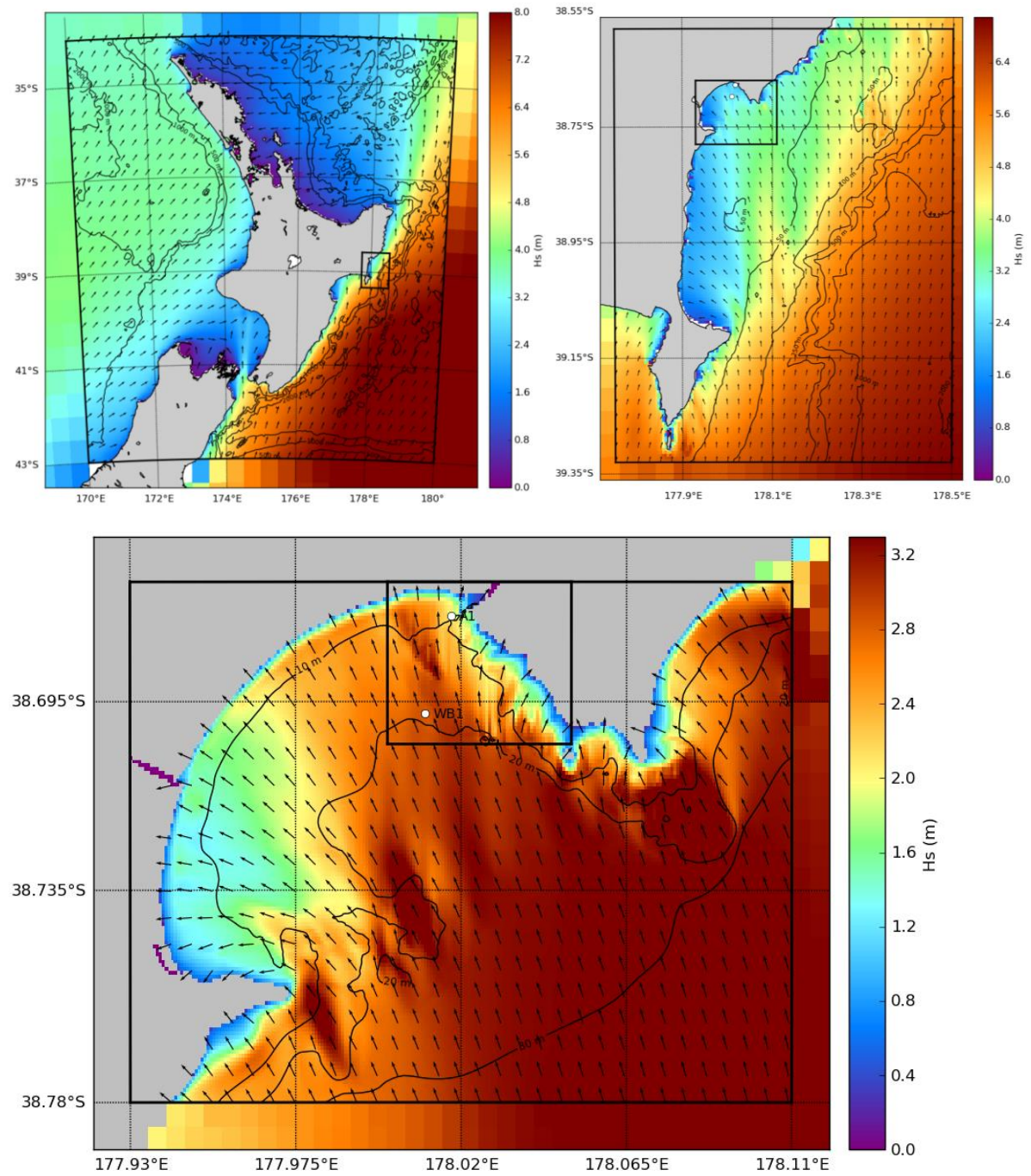


Figure 3.2. Snapshot of significant wave height from the NZN (res. 4km), Gisborne (res. 500m), and Poverty Bay (res. 80m) SWAN domains for a large southwest swell event (29 June 2012). The black rectangles show the successive nested domains.

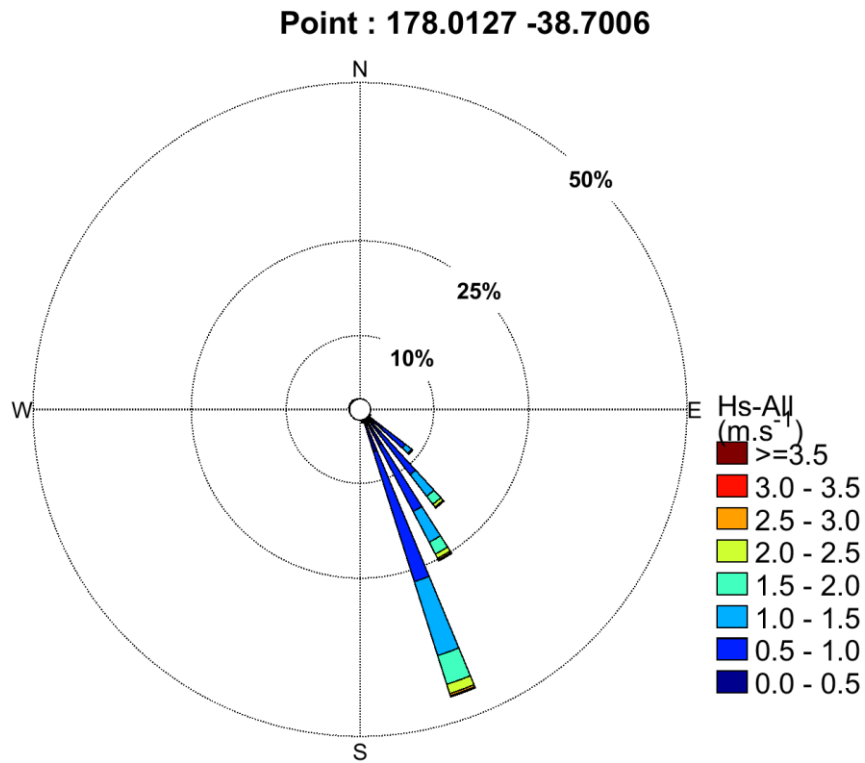


Figure 3.3. Mean wave rose over the 10 year time-series showing the distribution of significant wave heights and peak directions. Associated joint probabilities are provided in Table 3.1.

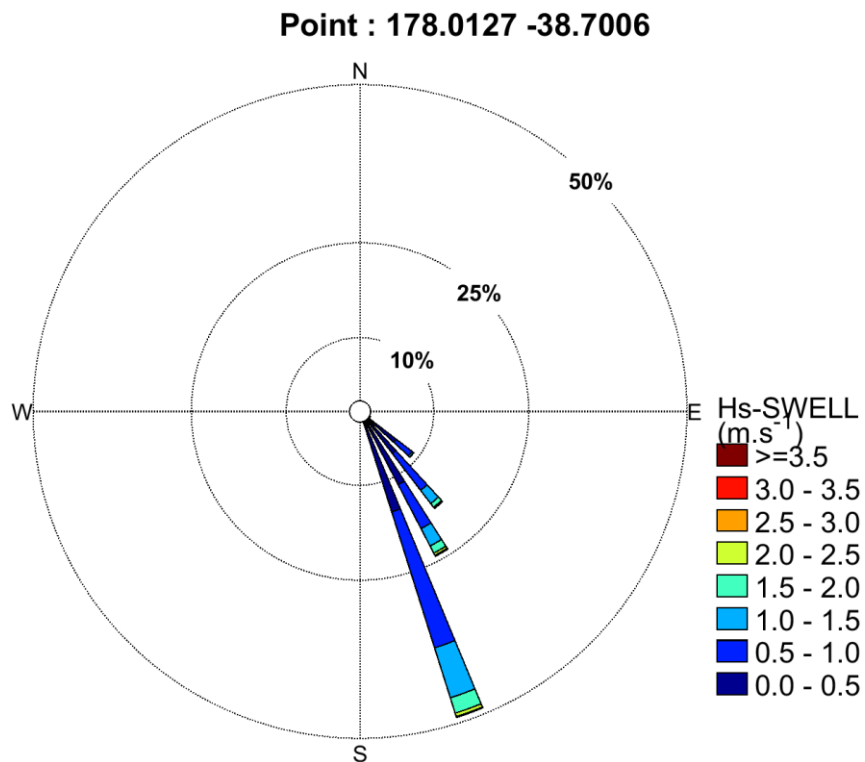


Figure 3.4. Mean wave rose over the 10 year time-series showing the distribution of significant swell wave heights and peak directions. Associated joint probabilities are provided in Table 3.2

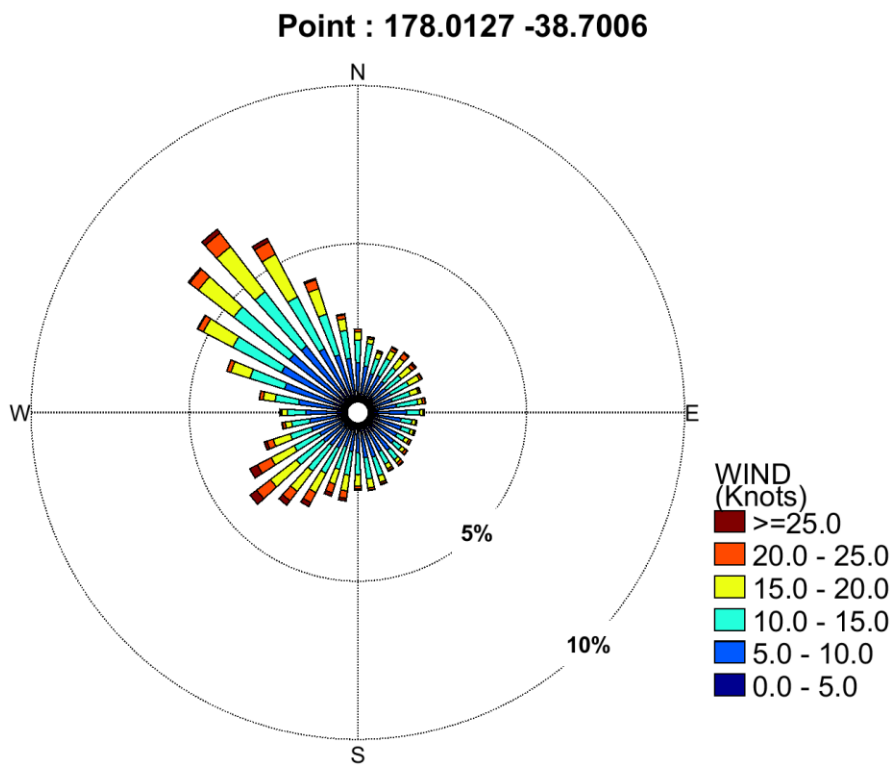


Figure 3.5. Mean wind rose over the 10 year time-series showing the distribution of significant wind speed and directions.

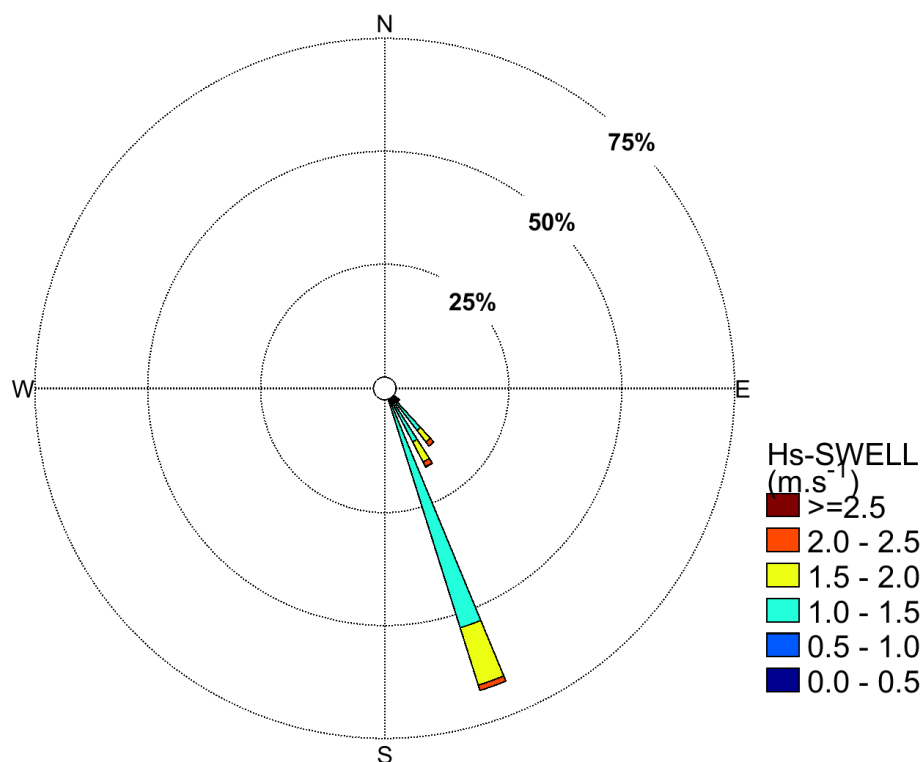


Figure 3.6. Wave rose for favourable surfing conditions during the 10 year time-series showing the distribution of significant swell wave heights and peak directions. Associated joint probabilities are provided in Table 3.3

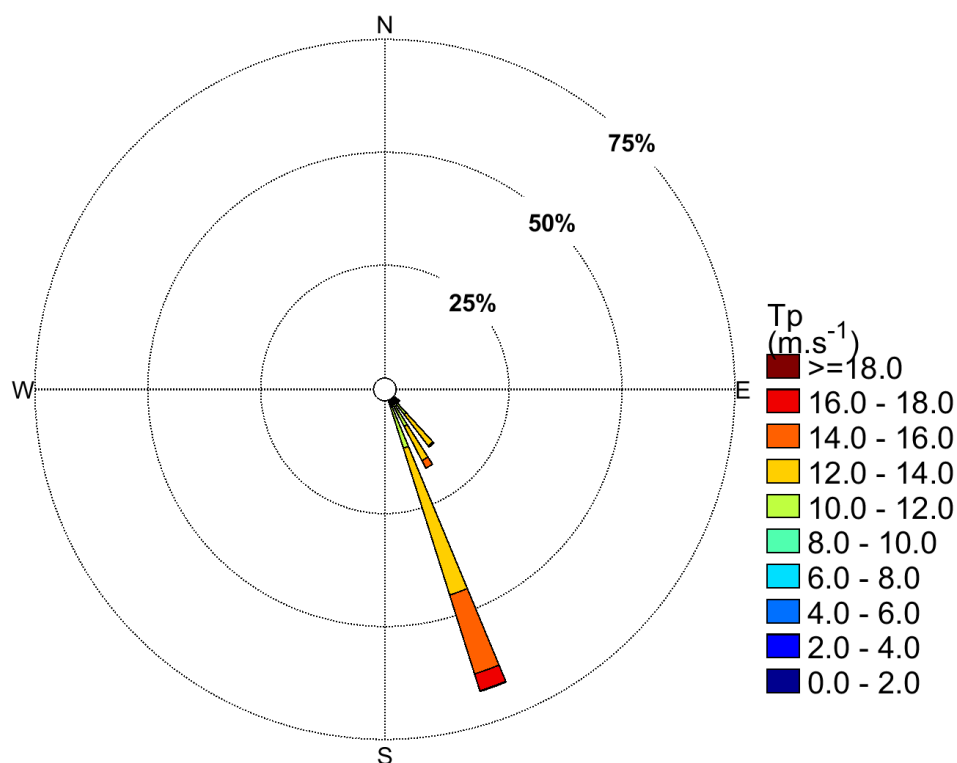


Figure 3.7. Wave rose for favourable surfing conditions during the 10 year time-series showing the distribution of peak periods and peak directions. Associated joint probabilities are provided in Table 3.4.

Table 3.1 Joint probabilities of significant wave heights and peak wave directions during the 10 year study period.

	120-130	130-140	140-150	150-160	160-170	170-180	180-190	190-200	200-210	210-220	220-230	230-240	240-250	250-260	260-270	270-280	280-290	290-300	300-310	310-320	320-330	330-340	340-350	350-360	SUM
0-0.5	14.3	31.9	34.8	76.2	3.6	0.2	0	0	0	0	0	0	0	0.1	0.2	0.6	1.2	0.7	1	0.7	0.8	0.5	0.2	0	167.2
0.5-1	13.2	80.3	78.6	270.2	22.8	0.9	0.1	0	0	0	0	0.1	0.1	0.3	0.2	0.5	0.5	0.5	1	0.7	0.8	0.5	0.1	0	471.4
1-1.5	0.9	36.7	39	143	14.2	0.2	0	0	0	0	0	0	0	0	0	0	0	0	0	0	0	0	0	0	234
1.5-2	0.1	10.2	15.3	55.3	5.8	0	0	0	0	0	0	0	0	0	0	0	0	0	0	0	0	0	0	0	86.7
2-2.5	0	2.4	5.9	19.2	1.1	0	0	0	0	0	0	0	0	0	0	0	0	0	0	0	0	0	0	0	28.7
2.5-3	0	0.4	2.4	4.8	0.2	0	0	0	0	0	0	0	0	0	0	0	0	0	0	0	0	0	0	0	7.7
3-3.5	0	0.1	0.9	2.1	0	0	0	0	0	0	0	0	0	0	0	0	0	0	0	0	0	0	0	0	0
3.5-4	0	0	0.2	0.7	0	0	0	0	0	0	0	0	0	0	0	0	0	0	0	0	0	0	0	0	0.9
4-4.5	0	0	0.2	0.1	0	0	0	0	0	0	0	0	0	0	0	0	0	0	0	0	0	0	0	0	0.3
4.5-5	0	0	0	0.1	0	0	0	0	0	0	0	0	0	0	0	0	0	0	0	0	0	0	0	0	0.1
5-5.5	0	0	0	0	0	0	0	0	0	0	0	0	0	0	0	0	0	0	0	0	0	0	0	0	0
5.5-6	0	0	0	0	0	0	0	0	0	0	0	0	0	0	0	0	0	0	0	0	0	0	0	0	0
SUM	28.5	162	177.2	571.7	47.7	1.3	0.1	0	0	0	0	0.1	0.1	0.3	0.4	1.1	1.7	1.2	2	1.4	1.6	1	0.3	0	1000

Table 3.2 Joint probabilities of significant swell wave heights (period>8 seconds) and peak wave directions during the 10 year study period.

	120-130	130-140	140-150	150-160	160-170	170-180	SUM
0-0.5	24.5	68.3	74.3	213.7	6.2	0	387
0.5-1	2.8	78.1	49.4	263	15.8	0	409.1
1-1.5	0	19.8	18.9	102.2	2.4	0	143.2
1.5-2	0	3.8	8.1	33.6	0.2	0	45.7
2-2.5	0	0.4	2.9	8.2	0	0	11.6
2.5-3	0	0	0.3	1.8	0	0	2.2
3-3.5	0	0	0.3	0.7	0	0	1
3.5-4	0	0	0.1	0.2	0	0	0.3
4-4.5	0	0	0	0	0	0	0
4.5-5	0	0	0	0	0	0	0
5-5.5	0	0	0	0	0	0	0
5.5-6	0	0	0	0	0	0	0
SUM	27.3	170.5	154.3	623.3	24.5	0	1000

Table 3.3 Joint probabilities of significant swell wave heights and peak wave directions during good surfing conditions (see surfing conditions criteria's in section 2.2).

	120-130	130-140	140-150	150-160	160-170	170-180	SUM
0-0.5	0	0	0	0	0	0	0
0.5-1	0	0	0	0	0	0	0
1-1.5	0	90.3	45.7	611.1	1.1	0	748.2
1.5-2	0	23.4	13.9	177.7	0	0	215
2-2.5	0	1.1	11.1	23.4	0	0	35.7
2.5-3	0	0	0	1.1	0	0	1.1
3-3.5	0	0	0	0	0	0	0
3.5-4	0	0	0	0	0	0	0
4-4.5	0	0	0	0	0	0	0
4.5-5	0	0	0	0	0	0	0
5-5.5	0	0	0	0	0	0	0
5.5-6	0	0	0	0	0	0	0
SUM	0	114.8	70.8	813.4	1.1	0	1000

Table 3.4 Joint probabilities of peak wave period and peak wave directions during good surfing conditions (see surfing conditions criteria's in section 2.2).

	120-130	130-140	140-150	150-160	160-170	170-180	SUM
2-3	0	0	0	0	0	0	0
3-4	0	0	0	0	0	0	0
4-5	0	0	0	0	0	0	0
5-6	0	0	0	0	0	0	0
6-7	0	0	0	0	0	0	0
7-8	0	0	0	0	0	0	0
8-9	0	0	0	0	0	0	0
9-10	0	0	0	0	0	0	0
10-11	0	0	0	0	0	0	0
11-12	0	42.3	23.4	164.3	1.1	0	231.2
12-13	0	53.5	32.3	200.6	0	0	286.4
13-14	0	18.4	11.7	206.1	0	0	236.2
14-15	0	0.6	1.7	133.7	0	0	135.9
15-16	0	0	1.7	68	0	0	69.6
16-17	0	0	0	29.5	0	0	29.5
17-18	0	0	0	9.5	0	0	9.5
18-19	0	0	0	1.7	0	0	1.7
19-20	0	0	0	0	0	0	0
SUM	0	114.8	70.8	813.4	1.1	0	1000

3.2. Nearshore wave modelling

3.2.1. Big River

The surf break Big River is situated approximately inshore of the offshore disposal ground (Figure 1.2), and as such the effect of the potential disposal mound on inshore wave characteristics has been assessed using the phase-averaging SWAN model (see Section 2.3).

The effect of the offshore disposal mound on the inshore wave climate considers the worst-case situation in which all the maintenance dredge material is deposited at once and does not undergo any adjustment associated with morphological response.

The maximum disposal mound associated with the maintenance dredging requirements expected under El Niño climatic conditions (i.e. worst case channel infilling and required maintenance dredging) is of the order 0.044 m, and has the potential to have a very slight effect on the inshore significant wave height (Figure 3.8 to Figure 3.13 for key classes as described in (MetOcean Solutions, 2018).

Due to wave refraction over the disposal mound, areas of slightly increased wave height are expected immediately inshore of the disposal ground, with the location of the wave height increase dependant on the incident wave direction. Conversely, areas of slightly reduced wave height are expected along each shore normal edge of the disposal ground and inshore, with the locations of reduced wave energy dependent on the incident wave direction (Figure 3.8 to Figure 3.13). In general, the wave height modifications are of the order 0.005 m, and a maximum increase of ~0.01 m and maximum decrease of 0.006 m. This corresponds to an approximate $\pm 0.2\%$ change in wave heights. The slight alteration to the wave climate is consistent with the water depth modification (~0.2%) related to the disposal of 120,000 m³ of sediment at the offshore disposal ground and is expected to have negligible effects on the inshore morphological processes and recreational surfing conditions at Big River.

Results presented assume no morphological changes to the disposal mound over the period the maintenance dredging is expected to occur. As such, presented results are considered to represent the worst-case outcome in terms of wave height modifications over the disposal mound and inshore. The volumetric response of the disposal mound is examined in MetOcean Solutions, (2018).

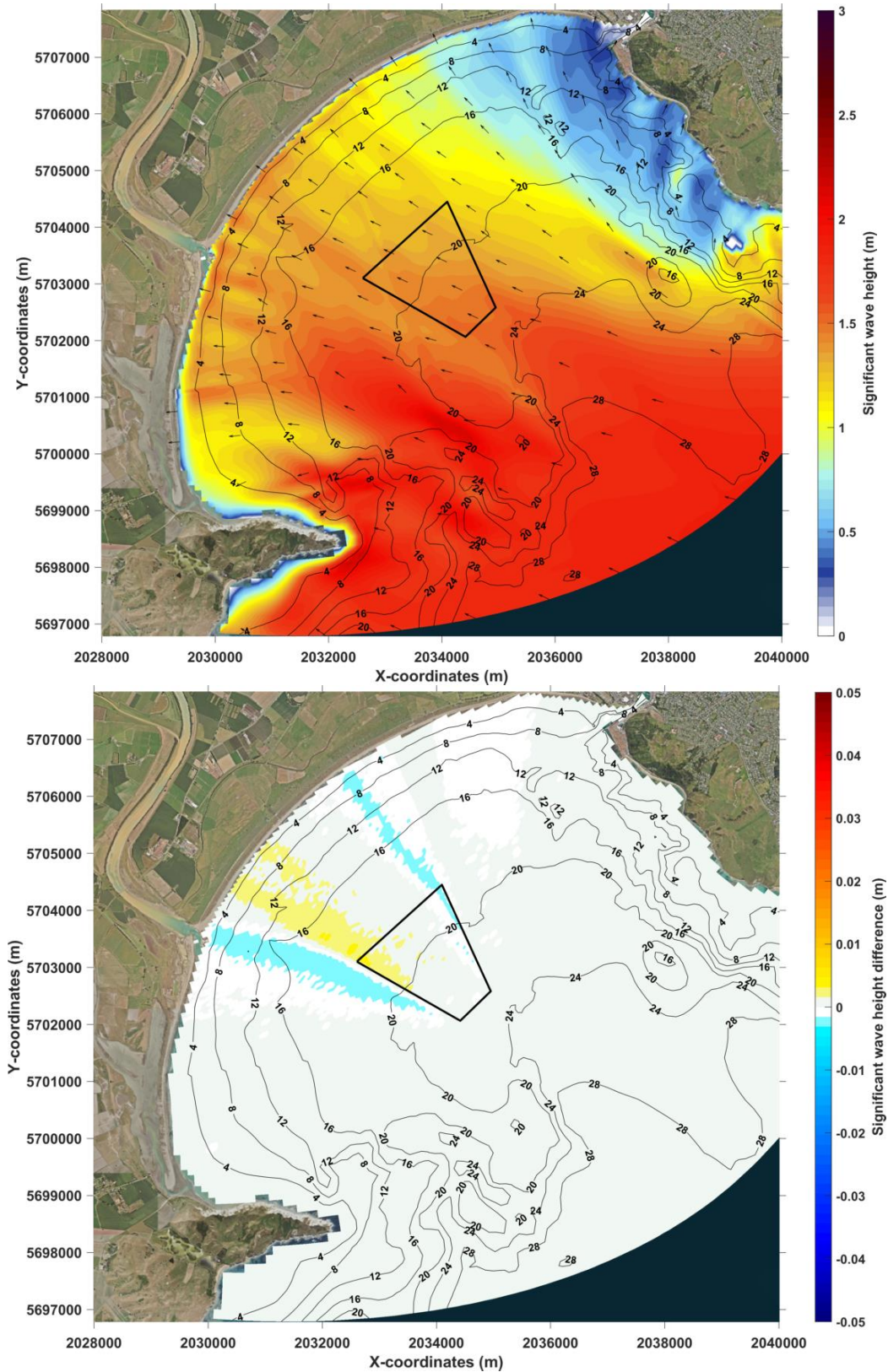


Figure 3.8 Post-disposal significant wave height (top) and difference in significant wave height (bottom) caused by the 4.4 cm disposal mound for the wave class 1.

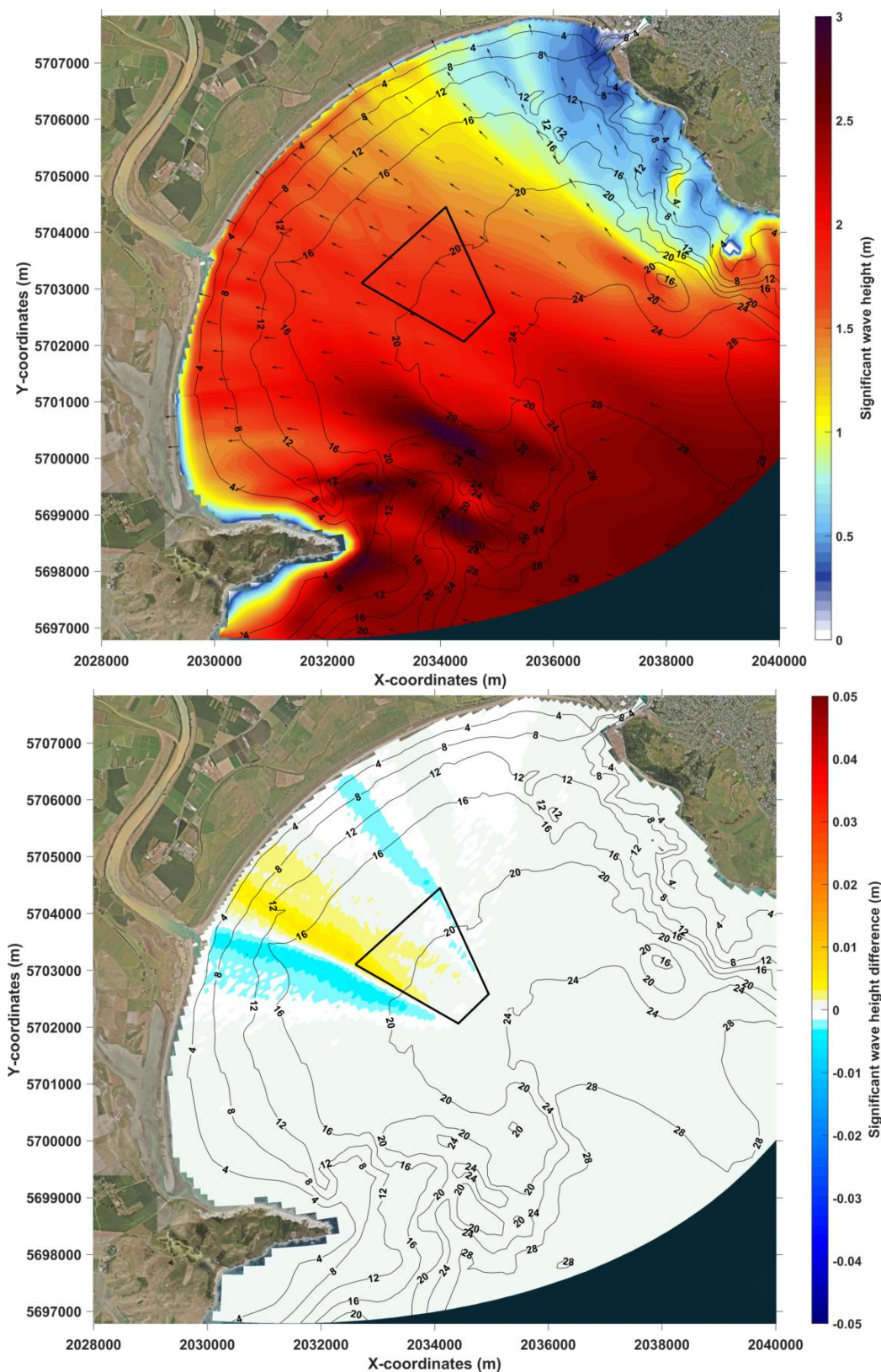


Figure 3.9 Post-disposal significant wave height (top) and difference in significant wave height (bottom) caused by the 4.4 cm disposal mound for the wave class 2.

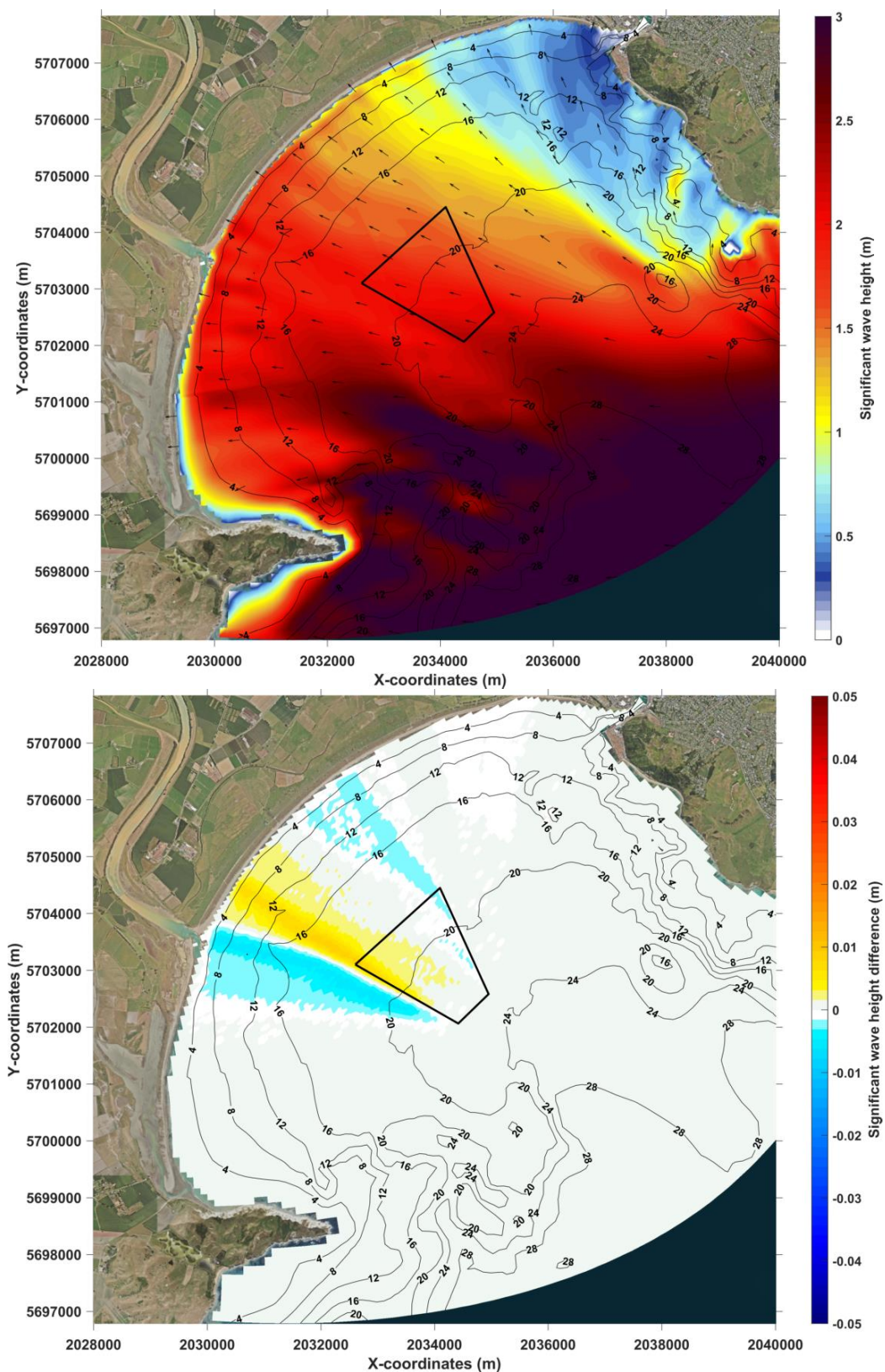


Figure 3.10 Post-disposal significant wave height (top) and difference in significant wave height (bottom) caused by the 4.4 cm disposal mound for the wave class 3.

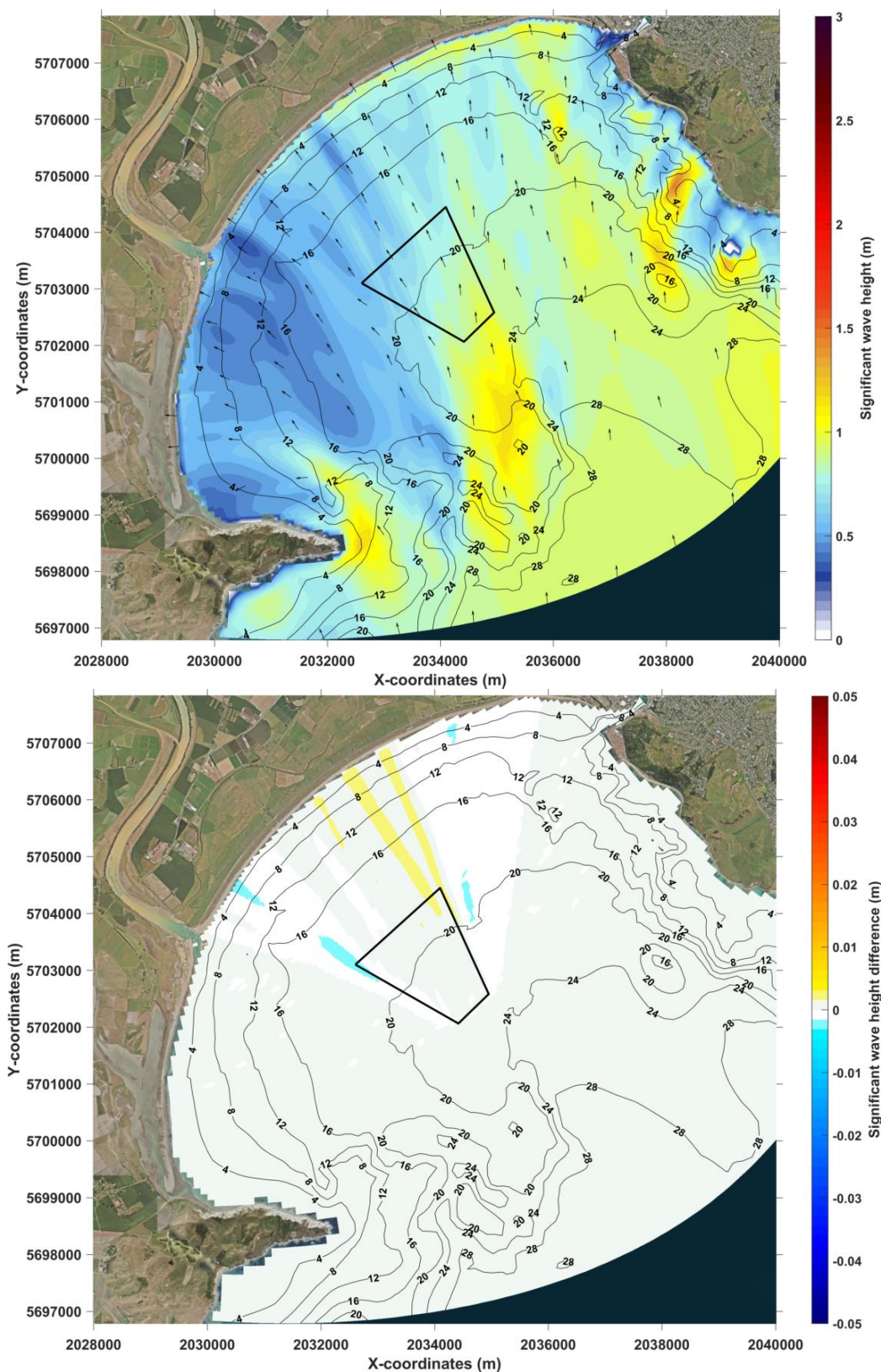


Figure 3.11 Post-disposal significant wave height (top) and difference in significant wave height (bottom) caused by the 4.4 cm disposal mound for the wave class 4.

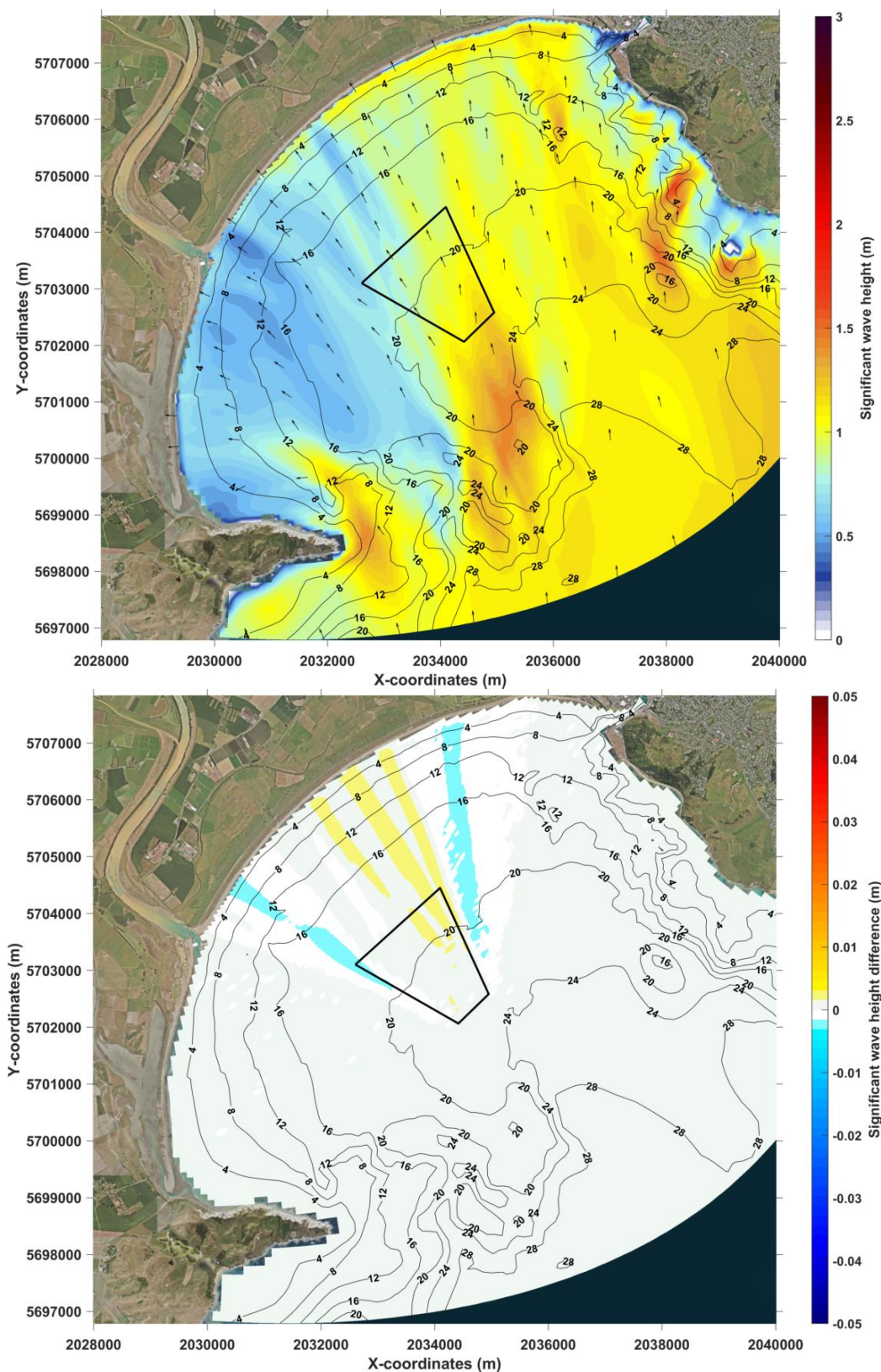


Figure 3.12 Post-disposal significant wave height (top) and difference in significant wave height (bottom) caused by the 4.4 cm disposal mound for the wave class 5.

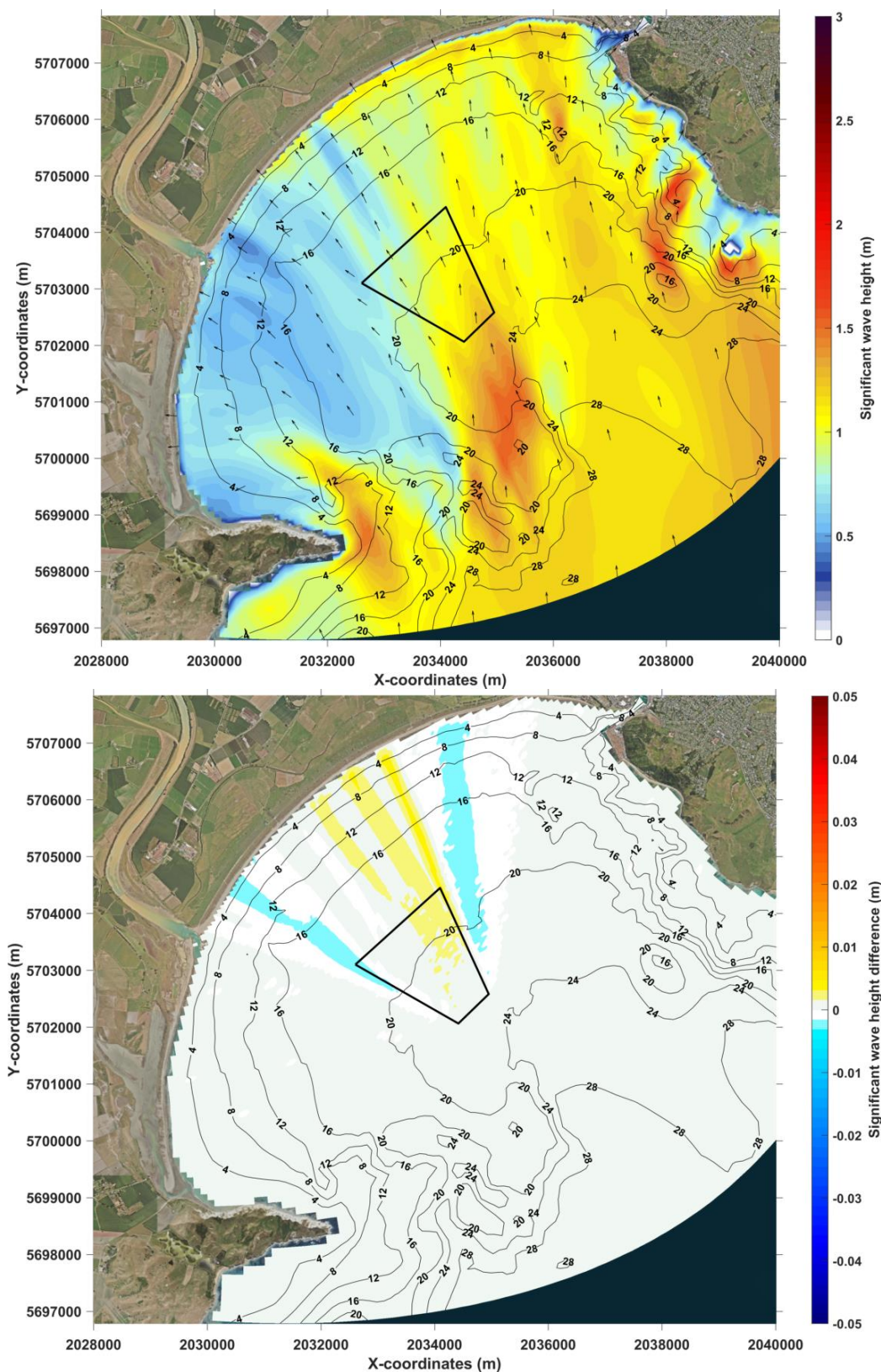


Figure 3.13 Post-disposal significant wave height (top) and difference in significant wave height (bottom) caused by the 4.4 cm disposal mound for the wave class 6.

3.2.2. Pipe and Roberts Road

Based on the surfing wave analysis (section 3.1), idealised surfing wave events with significant wave height of 2.0 meters, peak period of 12.0 seconds and incidence window from 140,150,160, and 170 deg T were considered for the nearshore wave modelling. Both monochromatic and spectral wave conditions were simulated. Monochromatic wave events represent “pure” swell conditions where only a single wave height, period and direction are assumed. These events are very useful to characterise the key wave patterns affecting inshore surfing conditions as the waves propagate over the seabed but are not fully realistic when compared to true sea states composed of a mixture of a multitude of superimposed waves with different heights, periods and directions (i.e. wave spectrum). Spectral wave simulations were also undertaken for the “best” incident wave direction for surfing at Midway Beach.

The modelling approach consists of reproducing the same wave simulations over the existing bathymetry (see Figure 2.2) and assessing relative modulations of the existing wave processes. The wave model was not specifically calibrated so the assessment remains qualitative.

Previous research on the site by Beamsley and Black (2003) identified significant wave focusing developing over offshore reefs in Poverty Bay which redirects enhanced wave energy specifically towards Midway Beach, and thus locally improved the inshore surfing conditions relative to adjacent beach stretches. The surfing wave improvement is attributed to the introduction of wave height gradients in the incident wave field thereby improving the wave peeling angles. The intense and local wave refraction developing over the reef can also allow distinct wave crest “snapping” thereby transmitting fragmented portions of wave crests, with phase offset, eventually creating highly surfable waves when reaching the shore i.e. so-called A-frames. Similar wave focusing processes are found at many high-quality surfbreaks such as Aramaona Beach in New Zealand (MetOcean Solutions Ltd, 2011), Matakana Island, Bay of Plenty, Stradbroke Island, Australia or Blacks in California (Magne, R. et al., 2007).

The results of the monochromatic wave simulations for the existing bathymetry are provided in Figure 3.14 to Figure 3.17. The wave focusing developing over the submerged reef system offshore of Midway Beach area is visible in all cases. For wave incidences in the 150-160°T range, which were identified as the most frequent swell conditions favourable for surfing (Figure 3.6, Table 3.3), the wave crests approach the reef system nearly perpendicularly. The reef systems result in intense wave focusing that redirects enhanced wave energy towards the Midway Beach area (red dot in plots). Local wave crest snapping features are also present in the water level snapshots.

The monochromatic simulations focusing on the functional features of the Midway Beach surfbreaks (Pipe, Roberts Road etc.) were supplemented by two spectral simulations of the “best” wave incidences. Standard JONSWAP spectra with significant wave height of 2.0 m and peak period of 12.0 seconds and peak directions of 150 and 160°T were simulated. Best surfing events typically have limited directional spreading (i.e. “clean swell”); here a value of 10 degrees was used. The spectral simulations allow reproducing more realistic sea states, comprised of a mix of many wave components with different height, periods and directions. They generally produce much smoother results when looking at relative wave height differences.

Snapshots of sea surface elevation and significant wave height fields are shown in Figure 3.18 and Figure 3.19 for the existing bathymetry. The wave crest focusing is expectedly less evident in the sea surface elevation snapshots relative to the monochromatic simulations, but it can still be identified over and in the lee of the submerged reef system off Midway Beach. The significant wave height fields do show a clear beam of larger wave height directed towards the Midway Beach area.

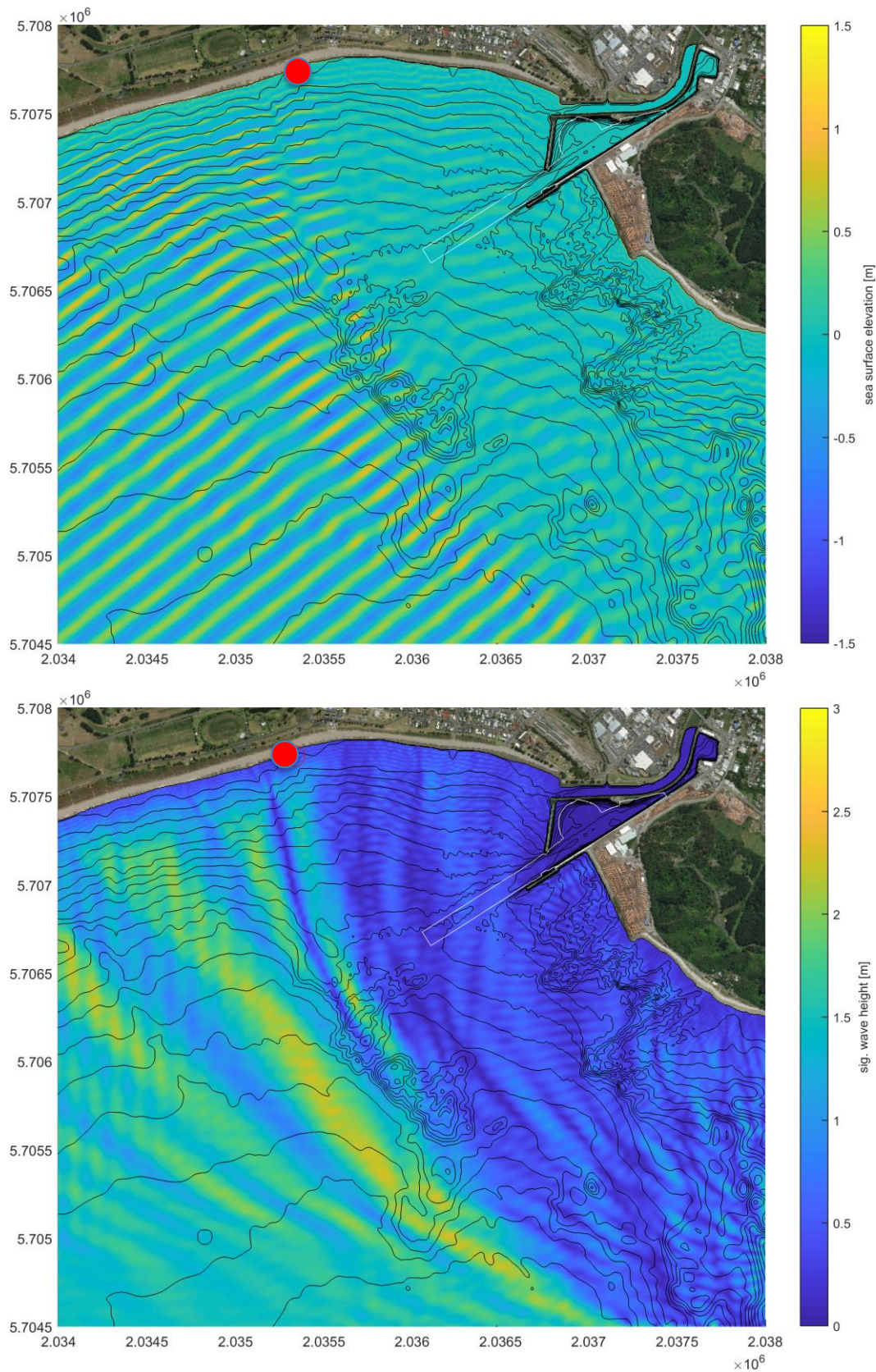


Figure 3.14 Snapshots of sea surface elevation (top) and significant wave height field (bottom) predicted for idealized monochromatic wave conditions $H_s = 2.0\text{m}$, $T_p = 12\text{ sec.}$ and $D_p = 140^\circ\text{T}$, over the existing bathymetry. The channel footprint is shown as a white polygon. The Midway Beach area is shown by the red dot.

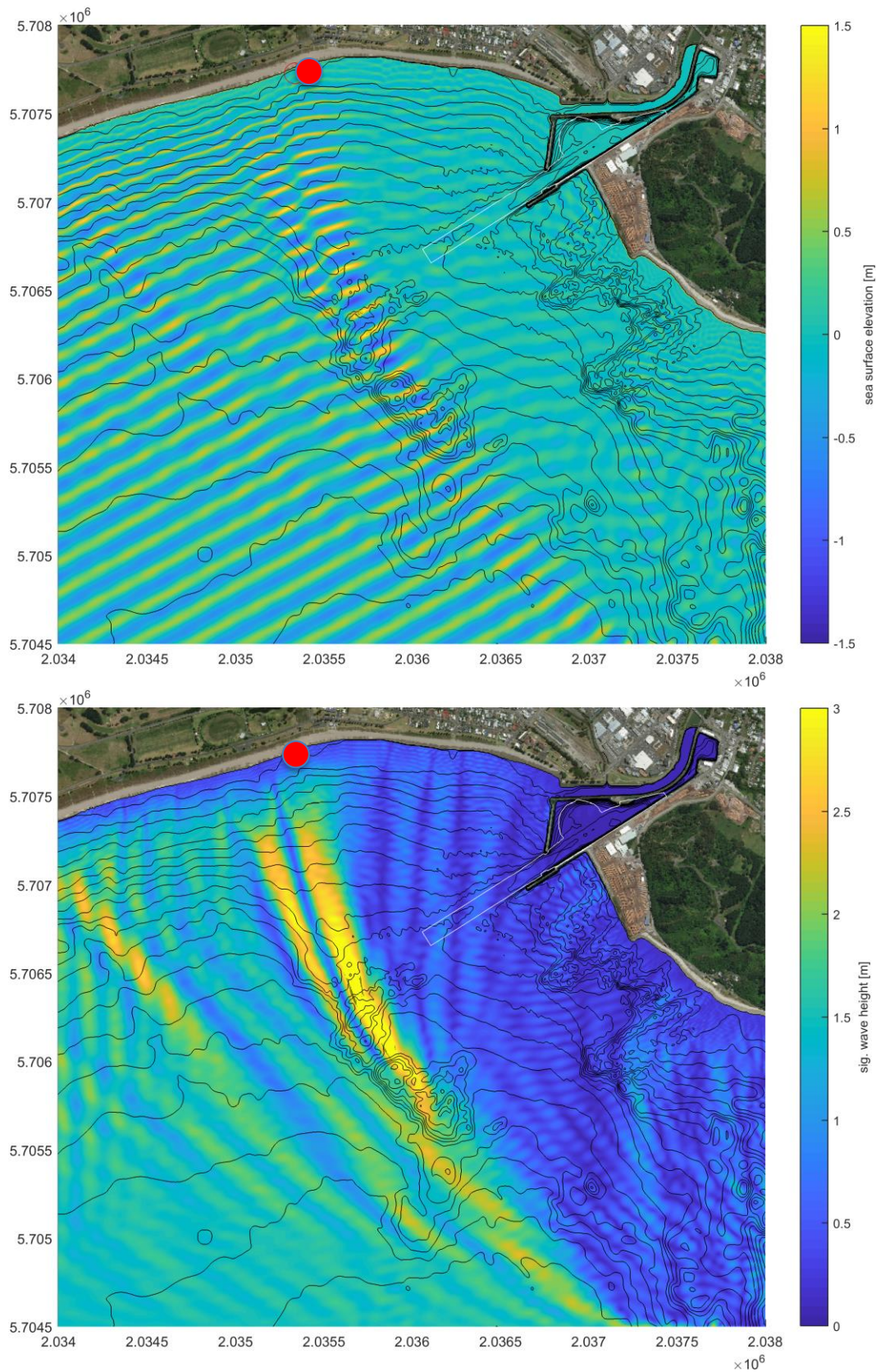


Figure 3.15 Snapshots of sea surface elevation (top) and significant wave height field (bottom) predicted for idealized monochromatic wave conditions $H_s = 2.0\text{m}$, $T_p = 12 \text{ sec.}$ and $D_p = 150^\circ\text{T}$, over the existing bathymetry. The channel footprint is shown as a white polygon. The Midway Beach area is shown by the red dot.

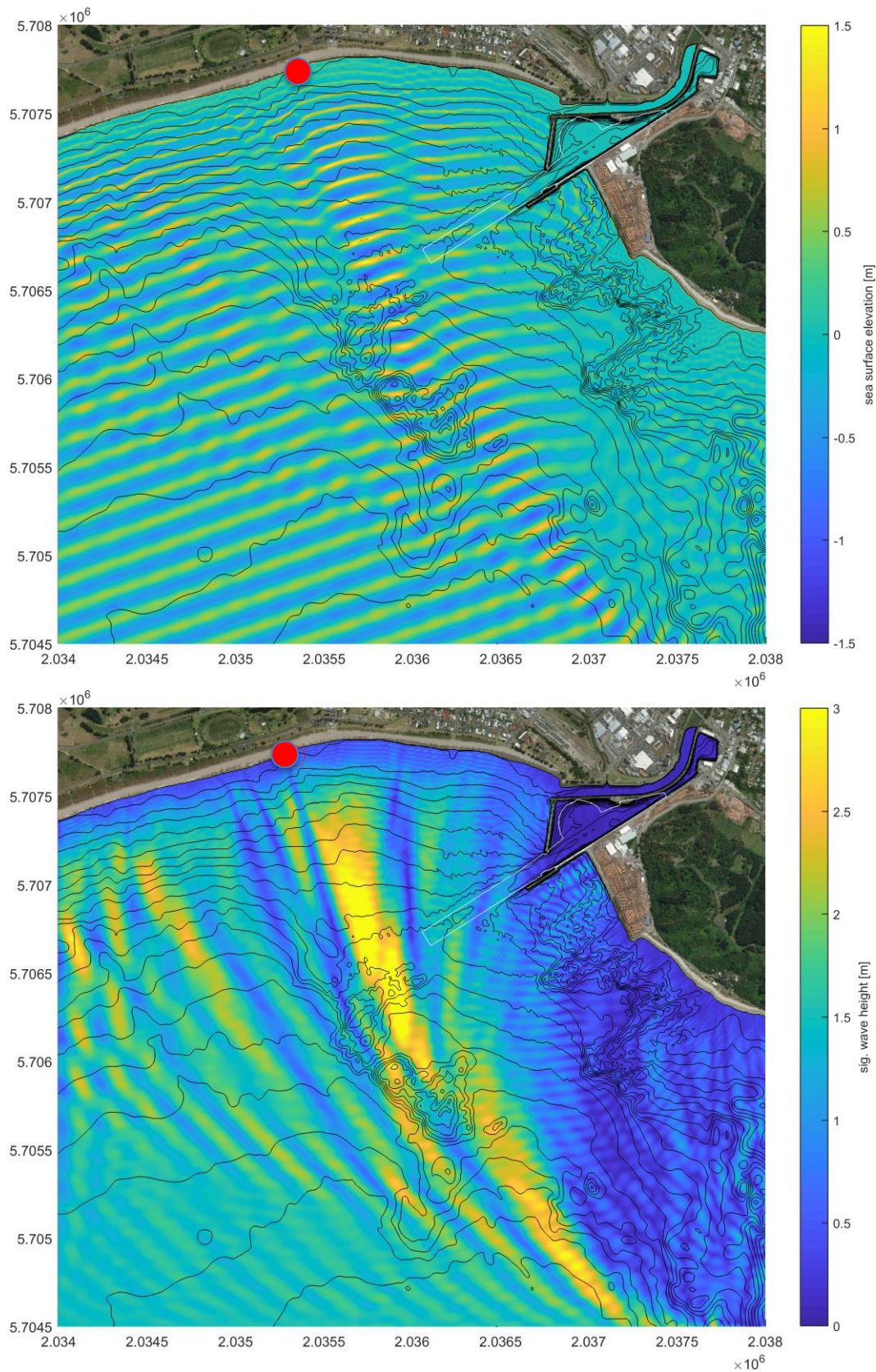


Figure 3.16 Snapshots of sea surface elevation (top) and significant wave height field (bottom) predicted for idealized monochromatic wave conditions $H_s = 2.0\text{m}$, $T_p = 12\text{ sec.}$ and $D_p = 160^\circ\text{T}$, over the existing bathymetry. The channel footprint is shown as a white polygon. The Midway Beach area is shown by the red dot.

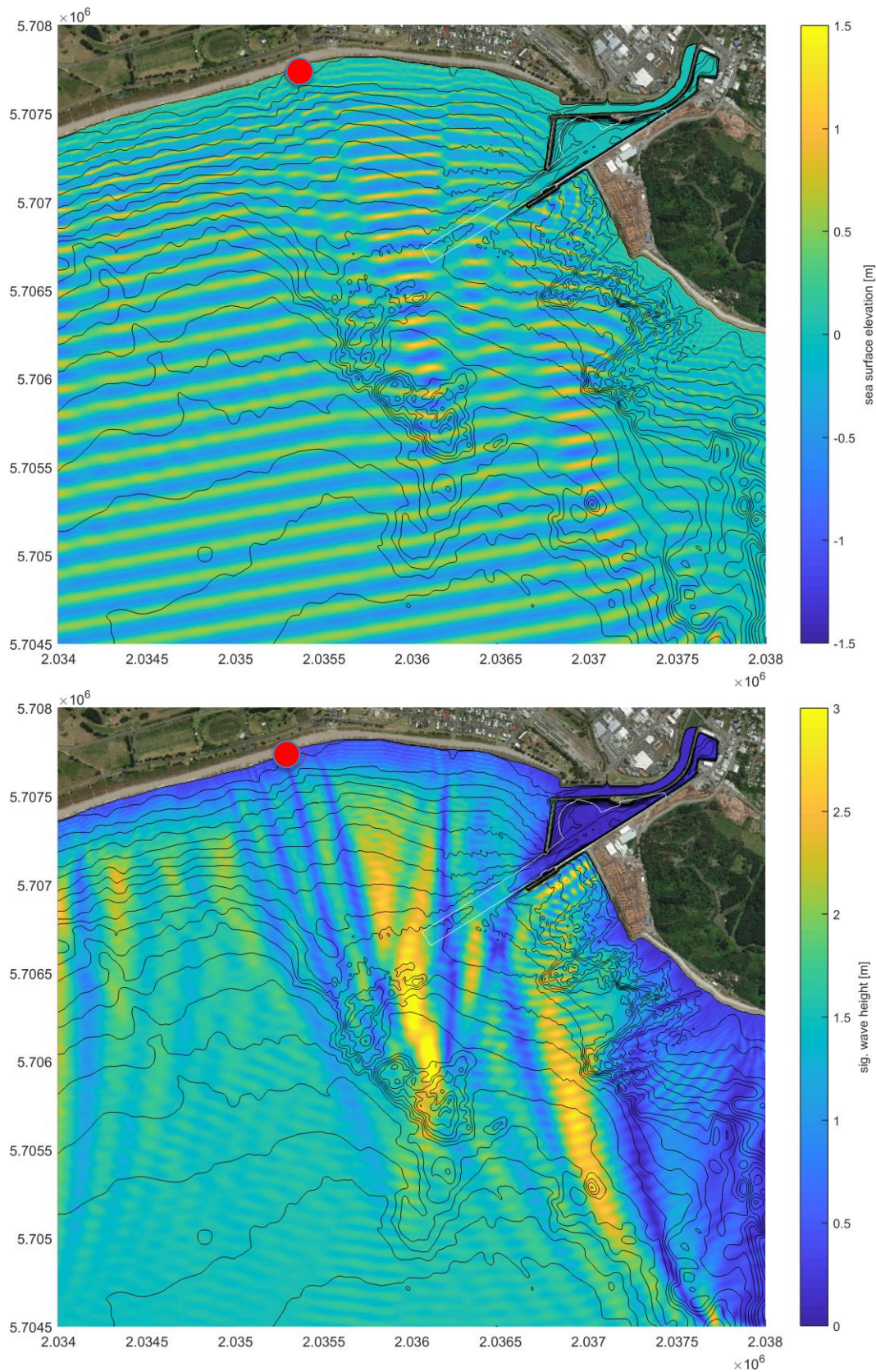


Figure 3.17 Snapshots of sea surface elevation (top) and significant wave height field (bottom) predicted for idealized monochromatic wave conditions $H_s = 2.0\text{m}$, $T_p = 12\text{ sec.}$ and $D_p = 170^\circ\text{T}$, over the existing bathymetry. The channel footprint is shown as a white polygon. The Midway Beach area is shown by the red dot.

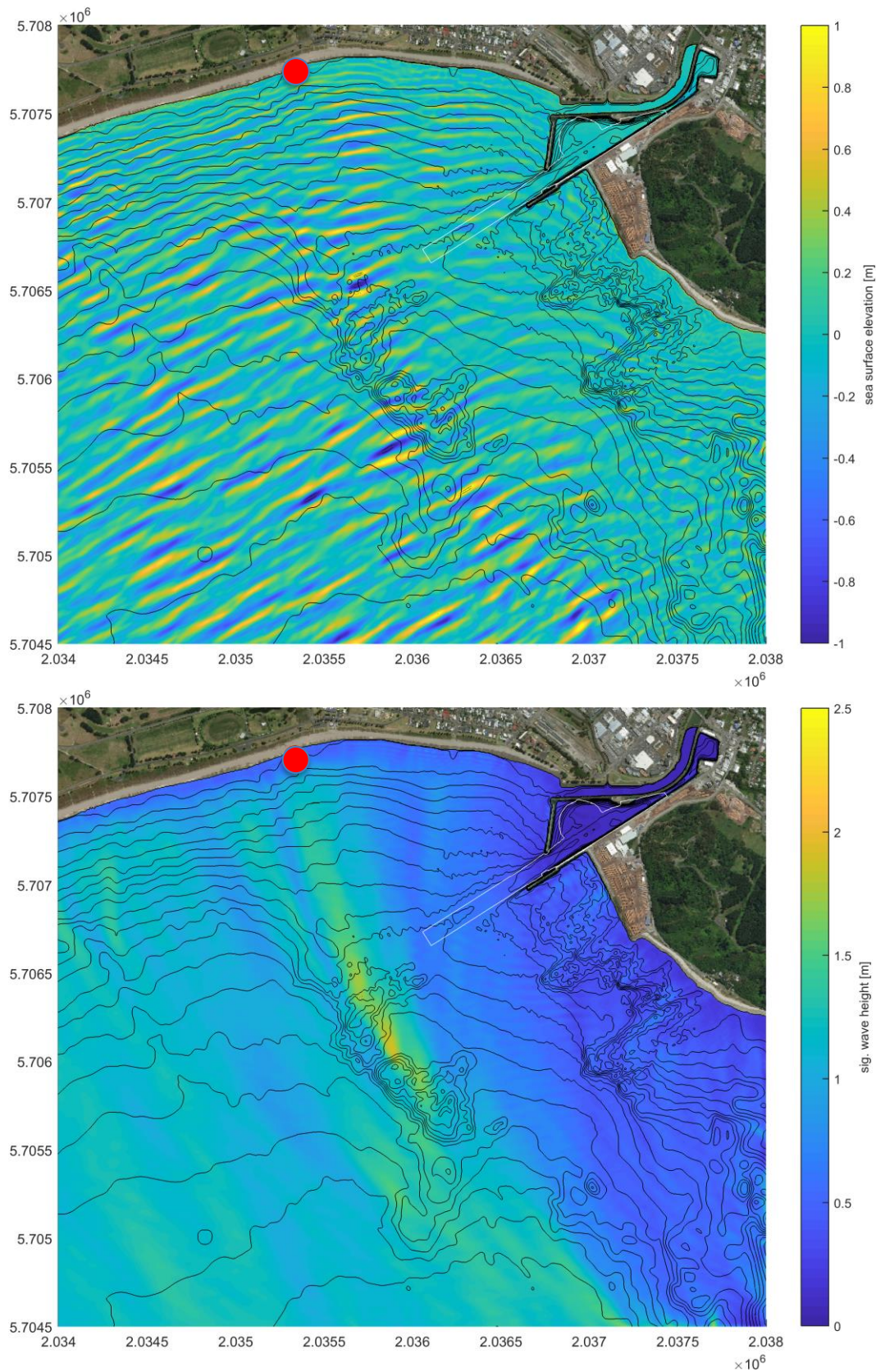


Figure 3.18 Snapshots of sea surface elevation (top) and significant wave height field (bottom) predicted for idealized spectral wave conditions $H_s = 2.0\text{m}$, $T_p = 12\text{ sec}$. and $D_p = 150^\circ\text{T}$, over the existing bathymetry. The channel footprint is shown as a white polygon. The Midway Beach area is shown by the red dot.

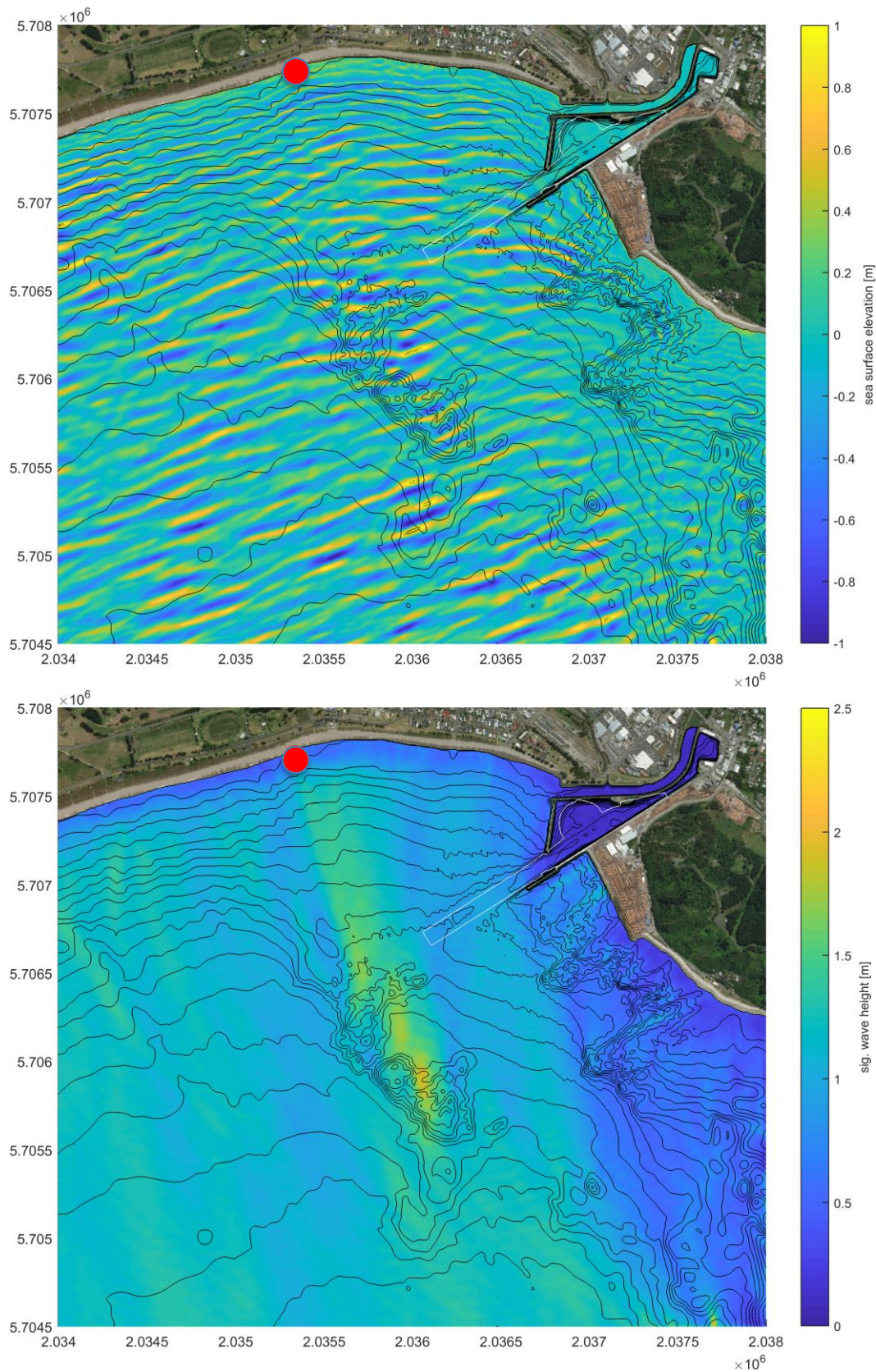


Figure 3.19 Snapshots of sea surface elevation (top) and significant wave height field (bottom) predicted for idealized spectral wave conditions $H_s = 2.0\text{m}$, $T_p = 12 \text{ sec.}$ and $D_p = 160^\circ\text{T}$, over the existing bathymetry. The channel footprint is shown as a white polygon. The Midway Beach area is shown by the red dot.

4. CONCLUSIONS

The study assesses the effects of the Eastland Port maintenance dredging and disposal project on the existing nearshore wave processes in Poverty Bay and specifically how maintenance dredging and disposal may affect the resulting wave conditions at the Midway Beach area (which has several notable surf spots, including Pipe and Roberts Road) and at the Waipaoa River mouth (i.e. Big River). Other Nationally and regionally significant surf breaks within Poverty Bay are not expected to be impacted by the continuation of the maintenance dredging and disposal activities.

An analysis of the wave climate was undertaken using a 10-year time-series of wave parameters extracted from a high-resolution wave hindcast implemented in a previous study to characterise the general wave climate and identify the conditions favourable for surfing events. Poverty Bay is exposed to a relatively narrow incidence wave angle window (140-170°T) due to refraction and diffraction processes around the bay headlands and as the waves propagate into the bay. A large majority (>80%) of swell-dominated events favourable for surfing conditions approach the sites with incidence directions between 150-160°T.

With respect to the surf break at the Waipaoa River (i.e. Big River), phase-averaging modelling was used to assess the potential effect of the offshore disposal mound on the inshore surfing conditions. Big River does not rely on any pre-conditioning of the incident wave fields, but rather is reliant on banks controlled by the high volume river which creates consistently moving sand and shingle banks (Morse and Brunskill, 2004). Modelling suggests that under worst case conditions (i.e. maximum disposal mound height and neglecting any potential morphological response) the inshore wave heights expected to be modified by an order of $\pm 0.2\%$, with the location dependent on the incident wave direction. This is expected to have a negligible effect on recreational surfing conditions at Big River (i.e. the increase/decrease in wave height not expected to exceed ~ 1 cm).

For these wave incidences, the nearshore phase-resolving wave propagation modelling illustrated that significant wave focusing develops over the offshore submerged reef system which redirects wave energy specifically towards the Midway Beach region. This is combined with wave crest “snapping” which is expected to further increase the surfability of the wave field reaching the beach.

The existing shipping channel and the associated maintenance dredging required to maintain the channel are expected to have only a less than minor impact on surfing along Waikanea and Midway beaches. This is attributed to the relatively small deepening of the outer channel (compared to what would be expected) and the approximate perpendicular angle of the channel relative to the incident wave direction. Further, the general channel footprint lies outside of the focused beam of wave energy developing during best, and most frequent, wave incidence for favourable surfing conditions at Midway Beach (150-160°T). Neither the maintenance dredging activities nor the shipping channel are expected to have any effect on surfing at Tuamotu Island or “The Island” (a nationally significant surf break as listed New Zealand Government, 2010).

5. REFERENCES

- Ardhuin, F., Rogers, E., Babanin, A.V., Filipot, J.F., Magne, R., Roland, A., Van Der Westhuysen, A., Queffelec, P., Lefevre, J.M., Aouf, L., et al. (2010). Semiempirical dissipation source functions for ocean waves. Part I: Definition, calibration, and validation. *Journal of Physical Oceanography* 40, 1917–1941.
- Beamsley, B.J., and Black, K.P. (2003). The Effect Of Offshore Reefs on Inshore Surfing Conditions. In *Proceedings of the 3rd International Surfing Reef Conference*, (Raglan, New Zealand), p.
- Collins, J. (1972). Prediction of Shallow Water Spectra. *Journal of Geophysical Research* 77, 2693–2707.
- Holthuijsen, L.H. (2007). *Waves in oceanic and coastal waters* (Cambridge University Press).
- Magne, R., Belibassakis, K., T. Herbers, Ardhuin F., O'Reilly W. C., and Rey V. (2007). Evolution of surface gravity waves over a submarine canyon. *Journal of Geophysical Research* 112.
- MetOcean Solutions (2017). *Eastland Port Maintenance Dredging and Disposal Project. Wave hindcast validation.*
- MetOcean Solutions (2018). *Eastland Port Maintenance Dredging and Disposal Project. Morphological model validation.*
- MetOcean Solutions (2019). *Eastland Port Maintenance Dredging and Disposal Project. Morphological response of the offshore disposal ground to maintenance dredging.*
- MetOcean Solutions Ltd (2011). *Aramoana Beach- Surfing Wave Dynamics (Technical report prepared for Port Otago Limited.)*
- Morse, P., and Brunskill, p. (2004). *New Zealand Surfing Guide* (Greenroom Surf Media).
- New Zealand Government (2010). *New Zealand Coastal Policy Statement, 2010.*
- Smit, P., Zijlema, M., and Stelling, G. (2013). Depth-induced wave breaking in a non-hydrostatic, near-shore wave model. *Coastal Engineering* 1–16.
- Tolman, H.L. (1991). A Third-Generation Model for Wind Waves on Slowly Varying, Unsteady, and Inhomogeneous Depths and Currents. *J. Phys. Oceanogr.* 21, 782–797.
- Van der Westhuysen, A.J., Zijlema, M., and Battjes, J.A. (2007). Nonlinear saturation-based whitecapping dissipation in SWAN for deep and shallow water. *Coastal Engineering* 54, 151–170.
- Zijlema, M., Stelling, G., and Smit, P. (2011). SWASH: An operational public domain code for simulating wave fields and rapidly varied flows in coastal waters. *Coastal Engineering* 992–1012.